# COVID-19 Puzzles: A Resolution

Tony Berrada*, Jerome Detemple†, and Marcel Rindisbacher‡

January 15, 2022

**Abstract**

This paper examines the economic impact of COVID-19 in an equilibrium framework. Our model combines two ingredients: (i) beliefs-dependent preferences for economic dynamics and (ii) stochastic SEIRD model with unpredictable birth and vaccine discovery events for disease propagation. We estimate the model based on economic time series and COVID-19 data. We show it explains the behaviors and levels of the S&P 500, the index volatility, the unemployment growth rate, the consumption growth rate and the number of new cases during the recent outbreak, while providing a good match for 25 unconditional moments of economic time series. Beliefs-dependency emerges as a critical ingredient for this comprehensive explanation of short term dynamics during the COVID-19 outbreak and of long run statistical properties.

**JEL Classification**: G13.

**Key Words**: COVID-19, SEIRD, SIP-LIFT, jumps, beliefs-dependent preferences, stock market, equity premium, volatility, correlation, consumption, unemployment.

*Geneva Finance Research Institute, University of Geneva, Bd. du Pont d'Arve 40, CH-1211 Geneva 4, Switzerland. Email: Tony.Berrada@unige.ch

†Questrom School of Business, Boston University, 595 Commonwealth Ave., Boston, MA 02215, United States. Email: detemple@bu.edu

‡Questrom School of Business, Boston University, 595 Commonwealth Ave., Boston, MA 02215, United States. Email: rindisbm@bu.edu

## 1. Introduction

The COVID-19 outbreak challenges economic theory on several grounds. It is characterized by a sharp decline in the consumption growth rate followed by a quick reversal. It features a rapidly declining stock market followed by a slower increase to levels commensurate with initial values. It displays episodes of large and fluctuating volatility in the market. This paper seeks to explain the magnitudes and patterns of these short run empirical regularities in an integrated epidemic-economy model consistent with moment properties of long run economic time series.

The outbreak took markets across the world by surprise. Although data from China showed clear and early evidence of rapid propagation and associated economic damage, markets initially failed to react, discounting the possibility of contagion across regions and continents. The rapid decrease in the US market, for instance, began on February 20, several months after the epidemic started to rage in China. The S&P500 reached its trough on March 23, about 30% below average levels during the first two months of 2020. The index took nearly 5 months to recover its February 20 level. In parallel, the VIX, a measure of market volatility, went from 15.56 on February 20 to a peak of 82.69 on March 16. It then progressively decreased to 24.52 on June 5, before spiking at 40.79 on June 11. A second spike occurred on September 3 following a short-lived downward adjustment. It has since evolved in the 25-40 range. Markets in other countries have experienced similar patterns although at different dates and over different periods.

The goal of this paper is to explain these phenomena, more specifically levels and patterns that have characterized US markets. A key question is whether the empirical evidence associated with COVID-19 is consistent with the predictions of a "finely-tuned" asset pricing model. By finely-tuned, we mean an asset pricing model explaining the long run behavior of financial markets, i.e., outside epidemic states. Given such a model, questions pertaining to the origins of economic fluctuations can be addressed. Are level adjustment patterns and volatility bursts the result of certain policy decisions or of natural disease propagation mechanisms? Do they reflect behavioral responses of economic agents? Are they tied to events unrelated to COVID-

19? Answers to these question may help to provide perspective on the scope and effectiveness of policy making.

For these purposes, we use the model with beliefs-dependent risk aversion (BDRA) in Berrada, Detemple and Rindisbacher (2018) as a starting point. This choice is motivated by the overall performance, static and dynamic, of the model. On the static front it provides a good match for 25 moment condition, e.g., unconditional estimates of the equity premium, stock market volatility and correlations between stock returns and growth rates of consumption and dividends. On the dynamic front it has attractive properties, e.g., spikes in model-implied recession probabilities coincide with NBER recession periods, model volatility tracks realized volatility, and the equity premium displays countercyclical behavior.

First, we extend the model to incorporate short term dynamics associated with a pandemic. This extension accounts for the unpredictable nature of pandemic events and vaccine discoveries, and for mitigating governmental policies. Pandemic uncertainty is modelled through a non-recurrent Markov chain with three possible regimes: no pandemic, pandemic and vaccine. Although the extension is built around the SEIRD model, any alternative pandemic propagation mechanism can be readily substituted without affecting the solution procedure and the main structural results. Of particular note is the fact that the extension produces closed form solutions for equilibrium quantities, including stock prices and volatilities, in spite of the unpredictability associated with the pandemic uncertainty.

Second, we estimate the model based on COVID-19 data, S&P 500 level and volatility data and long run time series for consumption, dividends, macro aggregates, and others. Estimation is carried out in two stages. In the first stage, the pre-pandemic stage, the economic model is estimated based on 25 moment conditions. Relative to prior literature based on the BDRA model, the estimation uses an augmented data set from 1957 to 2019. In the second stage, the pandemic stage, the disease propagation parameters and the parameters governing its effects on consumption, dividend and unemployment are estimated. Estimation is carried out so as to minimize the mean squared distance between model-implied and observed S&P 500 level,

index volatility, and number of new COVID-19 cases. The data set used for that purpose goes from January 2020 to July 2020.

Third, we document the performance of the model. There are two aspects. We first show that the model performs well regarding the quantities that were targeted in the estimation. Model-implied statistics are close to their empirical counterparts, both during the pre-pandemic period and the early stages of the outbreak. Pre-pandemic, the estimated model provides a good fit for 25 targeted moment conditions, confirming the results in Detemple et al (2018) for the longer data set. Intra-pandemic, it closely matches the number of new cases and the variations in volatility recorded during the COVID-19 outbreak, and it displays the asymmetric V-shape pattern of the S&P 500 while matching the trough. More significantly, we then show that it performs well relative to quantities that were not targeted in the estimation procedure, e.g., aggregate consumption, unemployment, and recessions. Specifically, it closely matches the level of the unemployment growth rate during the outbreak, and provides a good match for the consumption growth rate. The model-implied recession probability increases during the COVID-19 recession period declared by the NBER, and decreases immediately after it. Finally, it displays the behavior exhibited by a rolling average of the dividend growth rate, albeit with a lead. Crucially, BDRA is necessary for explaining the patterns observed in the data.

The paper relates to three branches of the literature. First, it generalizes recent contributions seeking to examine the impact of pandemics on equilibrium asset prices, e.g., Detemple (2022). It differs in that it (i) integrates an epidemiology propagation model into the model with BDRA preferences, (ii) allows for unpredictable events such as the outbreak of a pandemic and the discovery of a vaccine, (iii) includes volatility and correlations in the analysis and focuses not only on patterns but also levels, and (iv) estimates a version of the model allowing for time-dependent contamination rate and examines its performance. The estimated model fits the data well: on the economic front, it explains the magnitudes and patterns of volatility variations, unemployment and consumption fluctuations and S&P 500 adjustments during the COVID-19 outbreak.

Second, it contributes to the general equilibrium asset pricing literature. It extends, in particular, the BDRA model in Berrada, Detemple and Rindisbacher (2018) showing that market value and volatility inherit new components tied to the likelihood of occurrence of an outbreak and the likelihood of a vaccine discovery. Equilibrium formulas obtained are explicit allowing for easy estimation and simulation. It also complements earlier studies such as Merton (1973), Breeden (1979) and Cox, Ingersoll and Ross (1985), by incorporating an unexpected epidemic phenomenon into an equilibrium valuation framework.

Third, it connects to the growing literature dealing with the COVID-19 outbreak. Recent contributions have documented the empirical impact on the market, e.g., Gorsuch and Koijen (2020) and volatility, e.g., Cheng (2020). The present paper explains this empirical evidence, along with other aspects, in an equilibrium setting. It shows in particular that BDRA is essential for rationalizing the data. Other recent articles examine the role and impact of mitigation policies, e.g., Eichenbaum et al (2021), Jones et al (2021) and Hong et al (2021). The first study investigates the implications of individual decisions and government policies for disease propagation mechanisms and economic aggregates dynamics. The second one incorporates similar elements, but focuses on the implications of inefficient work-at-home policies, taking account of learning-by-doing and heterogeneity across sectors. The last one focuses on optimal mitigation policies of firms in a partial equilibrium setting with stochastic transmission rate, unpredictable vaccine discovery rate and fixed cost of mitigation. The scope of our contribution differs as we explain short run dynamics during the COVID-19 outbreak along with the long run behavior of economic variables in a setting with endogenous stochastic discount factor, unpredictable economic regimes and unpredictable pandemic events.

Section 2 presents the model and provides equilibrium formulas. Section 3 describes the estimation procedure and examines the fit to the data, both long term and during the early stages of the COVID-19 outbreak. Conclusions follow. Appendix A details the SEIRD model under a shelter-in-place (SIP) policy. Proofs are in Appendix B. Complementary results are in Appendix C.

## 2. Economic and Epidemiology Model

We extend the BDRA model in Berrada, Detemple and Rindisbacher (2018) to account for a pandemic outbreak triggered by an unpredictable initial infection event and a subsequent unpredictable vaccine discovery event.

### 2.1. A Time-Dependent and Stochastic SEIRD Model

The epidemic propagation is assumed to be driven by a SEIRD model with time-dependent infection rate $\beta$, unpredictable triggering event and unpredictable vaccination discovery event.

The population is split in five categories: susceptible ( $\mathcal{S}$ ), exposed ( $\mathcal{E}$ ), infectious ( $\mathcal{I}$ ), recovered ( $\mathcal{R}$ ), and deceased ( $\mathcal{D}$ ). Let $p_s, p_e, p_i, p_r, p_d$ be the fractions in each categories, where the sum equals $1$. The infectious population further splits in three groups: asymptomatic $p_i^{asy}$, symptomatic mild $p_i^{sm}$, and symptomatic severe $p_i^{ss}$, so that $p_i = p_i^{asy} + p_i^{sm} + p_i^{ss}$. The last two categories consist of mildly sick and severely sick individuals, respectively. We assume $p_i^{ss} = p_i\lambda$, $p_i^{asy} = p_i(1-\lambda)\lambda_w$, $p^{sm} = p_i(1-\lambda)(1-\lambda_w)$ where fractions $\lambda$ and $\lambda_w$ are constants. Before the initial infection event, $p_s = 1$ and $p_e = p_i = p_r = p_i^{asy} = 0$. At the initial infection event date $\tau_0$, the infectious population jumps up and the susceptible population down: $\Delta p_{i\tau_0} > 0$ and $\Delta p_{s\tau_0} = -\Delta p_{i\tau_0} < 0$. Thereafter populations evolve as

$$dp_s = (\mu(1-p_d-p_s) - \beta(t)p_s p_i^{asy} - (\nu^o + \nu 1_{\mathcal{V}_t})p_s)dt \tag{2.1}$$

$$dp_e = (\beta(t)p_s p_i^{asy} - (\mu+\sigma)p_e)dt \tag{2.2}$$

$$dp_i = (\sigma p_e - (\mu+\mu_i+\gamma)p_i)dt \tag{2.3}$$

$$dp_r = (\gamma p_i - \mu p_r + (\nu^o + \nu 1_{\mathcal{V}_t})p_s)dt \tag{2.4}$$

$$dp_d = \mu_i p_i dt \tag{2.5}$$

where the indicator $1_{\mathcal{V}_t}$ indicates a pandemic has occurred and a vaccine has been found. The parameter $\beta(t)$ is the disease transmission rate, a function of time, $\sigma$ is the incubation rate, $\gamma$ the recovery rate, $\nu^o$ is the natural immunity rate, and $\nu$ is the vaccination rate upon

discovery of a vaccine. The birth and natural death rates $\mu$ are assumed to be equal, hence ensuring a stable population in the absence of disease mortality. Incremental disease mortality is $\mu_i$, and individuals who die as a result of the pandemic are in $\mathcal{D}$. All parameters, except for $\beta(t)$ are constants. The specific form of $\beta(t)$ is described in Section 3.2.1.

A policy intervention such as shelter-in-place (SIP) modifies the dynamics as follows. First, upon implementation, it introduces an outflow at rate $q$, called the compliance rate, in each of the populations above to corresponding sheltered populations $p_s^Q, p_e^Q, p_i^Q, p_r^Q, p_d^Q$, identified by the superscript $Q$. Second, upon lifting (LIFT) of the policy, it induces a reverse flow from sheltered populations to those that are not. This reverse compliance rate is $q_2$. In the sequel we refer to this model as the SEIRD-SIP-LIFT model. Details of the model can be found in Appendix A.

## 2.2. Regimes, Consumption, Dividends, and Information

We assume there are six regimes: expansion, recession, boom, no pandemic, pandemic and vaccine. The first three regimes are unobservable. They are the outcomes of a Markov chain $s_t^m$ with three states, recession ( $s_t^m = e_1$ ), expansion ( $s_t^m = e_2$ ) or boom ( $s_t^m = e_3$ ), where $e_k$ is the $3 \times 1$ -dimensional $k^{th}$ unit vector. The last three are observable and are the outcomes of an independent Markov chain $s_t^e$ with three states, no pandemic ( $s_t^e = e_1$ ), pandemic ( $s_t^e = e_2$ ) or vaccine ( $s_t^e = e_3$ ). The pandemic Markov chain is non-recurrent: it evolves from state $e_1$, to $e_2$, then $e_3$, which is an absorbing state. The vaccine event $1_{\mathcal{V}} = 1$ is triggered when $s_t^e = e_3$. In this event, the dynamics of the susceptible and infectious populations depend on the vaccination rate $\nu$ as described in $p_s$ and $p_r$. To simplify derivations we assume the pandemic is a one-time event, so does not subsequently reoccur: $s_t^e = e_3$ is an absorbing state.

To model the Markov chains, consider independent continuous-time switching process $(s^m, s^e)$

$$ds_t^m = \left(\Lambda^m dt + d\tilde{N}_t^m\right)' s_{t-}^m \tag{2.6}$$

$$ds_t^e = \left(\Lambda^e dt + d\tilde{N}_t^e\right)' s_{t-}^e \tag{2.7}$$

where $d\tilde{N}_t^\alpha = dN_t^\alpha - \Lambda^\alpha dt$ for $\alpha \in \{m, e\}$ and $N^\alpha$ is $3 \times 3$-matrix valued Poisson processes with independent off-diagonal elements, diagonal elements $dN_{iit} = -\sum_{j \neq i} dN_{ijt}$, and intensity matrix $\Lambda^\alpha$ with diagonal elements $\Lambda_{ii}^\alpha = -\sum_{j \neq i} \Lambda_{ij}^\alpha$. Each process takes values $s_t^\alpha \in \{e_i; i = 1, 2, 3\}$ where $e_i'$ denotes the $i^{th}$ unit vector. Define the different states as follows: expansion $s_t^m = e_1$, recession $s_t^m = e_2$, boom $s_t^m = e_3$, no pandemic $s_t^e = e_1$, pandemic $s_t^e = e_2$, pandemic and vaccine $s_t^e = e_3$. A pandemic arises with intensity $\Lambda_{12}^e$. As the development of a vaccine takes some time $\Lambda_{13}^e = 0$. If there is a pandemic $\Lambda_{21}^e = 0$. The vaccine enters development and becomes available with intensity $\Lambda_{23}^e$. Once it becomes available the pandemic ends, $\Lambda_{31}^e = \Lambda_{32}^e = 0$. The initial event triggering the pandemic is determined by the jump of $s_t^e$ to $e_2$. The vaccine event resolving the pandemic is determined by the jump to $e_3$.

The state variables in the model are $(C, G, Y)$ where $C$ is aggregate consumption and $(G, Y)$ are orthogonalized variables constructed from consumption, dividend and unemployment; see Appendix B for details. The model for $(C, G, Y)$ is

$$\frac{dC_t}{C_t} = \left(\mu_o^C(s_t^m) + A^C(s_t^m)\frac{\mu^{p_w^e}(t, s_t^e)}{p_{wt}^e}1_{\mathcal{E}_t}\right)dt + \sigma^C dW_t^C \tag{2.8}$$

$$\frac{dG_t}{G_t} = \left(\mu_o^G(s_t^m) + A^G(s_t^m)\frac{\mu^{p_w^e}(t, s_t^e)}{p_{wt}^e}1_{\mathcal{E}_t}\right)dt + \sigma^G dW_t^G \tag{2.9}$$

$$\frac{dY_t}{Y_t} = \left(\mu_o^Y(s_t^m) + A^Y(s_t^m)\frac{\mu^{p_w^e}(t, s_t^e)}{p_{wt}^e}1_{\mathcal{E}_t}\right)dt + \sigma^Y dW_t^Y \tag{2.10}$$

where $A^C(s_t^m), A^G(s_t^m), A^Y(s_t^m)$ are sensitivity parameters capturing the response to the epidemic, $\mu_t^{p_w^e}$ is the drift of the effective labor force $p_w^e$ generated by the SEIRD model (see end of next section for details), and $1_{\mathcal{E}_t}$ is the indicator of an epidemic outbreak $\mathcal{E}_t = \{s_t^e \in \{e_2, e_3\}\}$. The processes $W^C, W^G, W^Y$ are independent Brownian motions representing economic shocks. The terms $\left(\mu_o^C(s_t^m), \mu_o^G(s_t^m), \mu_o^Y(s_t^m)\right)$ represent the respective drifts in the absence of an epidemic. The terms involving $\frac{\mu^{p_w^e}(t, s_t^e)}{p_{wt}^e}$ capture the impact of the pandemic on the expected growth rates of $(C, G, Y)$. These components kick in either when an outbreak is in process $s_t^e = e_2$, or when it has already occurred and a vaccine has been found $s_t^e = e_3$. The model

(2.8)-(2.10) is a generalization of the reduced form suggested by the pandemic production model in Detemple (2022); it generalizes that specification by allowing for additional state variables $(G, Y)$ and for a dependence on the economic regime $s^m$ .

## 2.3. Beliefs-Dependent Risk Aversion: BDRA(K,K)

To model economic processes during a pandemic, we extend the BDRA(K,K) model in Berrada, Detemple and Rindisbacher (2018). The model has $K$ unobserved economic regimes $s_k^m : k = 1, ..., K$ , $K$ preference parameters $R_k : k = 1, ..., K$ and uses consumption $C$ , orthogonalized dividends $G$ and orthogonalized macro variables $Y$ as information sources. Let $P_k : k = 1, ..., K$ be the regime probabilities based on public information. Instantaneous utility of consumption, for population $j$ , is $u_j(c_t, t) = e^{-\beta_u t} \sum_{k=1}^K P_{kt} a_j^{R_k} c_t^{1-R_k}/(1 - R_k)$ where $\beta_u$ is a subjective discount rate and $a_j < 1$ is a discount factor depending on the health and employment status of the population. The coefficients $R_k$ are parameters of the risk aversion function, as explained below. Marginal utility of consumption is

$$u_{jc}(c_t, t) = e^{-\beta_u t} \sum_{k=1}^K P_{kt} \left(\frac{c_t}{a_j}\right)^{-R_k}, \qquad j \in \{s, e, i, r\} \tag{2.11}$$

and depends on the ratio of consumption to discount factor. Relative risk aversion is $R_j = \sum_{k=1}^K q_{jkt} R_k$ where $q_{jkt} = \frac{P_{kt} a_j^{R_k} c_t^{-R_k}}{\sum_{k=1}^K P_{kt} a_j^{R_k} c_t^{-R_k}}$ , different across populations for a given consumption level $c_t$ . As shown in the next section, equilibrium is completely determined by the dynamics of $(C, G, Y, P)$ , such that

$$dP_{kt} = P_{kt} \left(\mu_{kt}^p dt + \Delta_{kt}^C d\nu_t^C + \Delta_{kt}^G d\nu_t^G + \Delta_{kt}^Y d\nu_t^Y\right) \tag{2.12}$$

where $\mu_{kt}^p = \sum_{j=1}^K P_{jt} \lambda_{jk}/P_{kt}$ with $\lambda_{jk}$ the transition intensity from regime $j$ to $k$ , and for $\alpha \in \{C, G, Y\}$

$$\Delta_{kt}^\alpha = \frac{\mu_k^\alpha - \hat{\mu}_t^\alpha}{\sigma^\alpha}, \qquad d\nu_t^\alpha = \frac{1}{\sigma^\alpha}\left(\frac{d\alpha_t}{\alpha_t} - \hat{\mu}_t^\alpha dt\right), \qquad \frac{d\alpha_t}{\alpha_t} = \mu^\alpha(s_t)dt + \sigma^\alpha dW_t^\alpha \tag{2.13}$$

where $\mu^\alpha(s_t) = \mu^\alpha(s_t^m, s_t^e) = \mu_o^\alpha(s_t^m) + A^\alpha(s_t^m)\frac{\mu^{p_w^e}(t,s_t^e)}{p_w^e}1_{\mathcal{E}_t}$ , $\mu_k^\alpha = \mu^\alpha(s_t^m, s_t^e)_{s_t^m=e_k}$ , and $\hat{\mu}_t^\alpha = \sum_k \mu_k^\alpha P_k$ . The processes $\nu^C, \nu^G, \nu^Y$ are informational innovations associated with the underlying Brownian motions.

We also assume the supply of labor by households is inelastic. Aggregate labor supply is $\bar{L} = 100$ in the absence of an epidemic. During an outbreak available supply is limited to individuals who do not exhibit symptoms: the workforce is $p_w = p_s + p_e + p_i^{asy} + p_r$ . If SIP is implemented, and a fraction $h$ of quarantined individuals is able to work at home, the effective labor supplied is $p_w^e = p_w + \omega p_w^q$ where $\omega < 1$ is an efficiency factor and $p_w^q = p_{s,h}^q + p_{e,h}^q + p_{i,h}^{q,asy} = h\,(p_s^q + p_e^q + p_i^{q,asy})$ is the sheltered population able to work. The effective workforce impacts the growth rate of aggregate variables as described in (2.8)-(2.10).

The model combining the pandemic and economic dynamics described above is called the BRDA-SEIRD-SIP-LIFT model.

## 2.4. Equilibrium

The consumption demand of population $j$ is $c_{jt} = a_j I(H_t)$ for a function $I$ commmon to all populations and where $H_t = y\xi_t/a_t$ is the normalized state price density. Aggregate demand is $p_{ct}^a I(H_t)$ where $p_{ct}^a = \sum_{j\in\{s,e,i,r\}} p_{jt}a_j$ .[1] In equilibrium $p_{ct}^a I(H_t) = C_t$ so that $I(H_t) = C/p_{ct}^a$ . The equilibrium allocation satisfies $c_{jt}/a_j = I(H_t) = C_t/p_{ct}^a$ , which is identical across populations.

Let $\tau_0 \equiv \inf\{v \geqslant 0 : \Delta N_{12v}^e > 0\}$ be the time marking the beginning of the pandemic. At that time the infectious population becomes positive, $\Delta p_{i\tau_0} > 0$ , and all quantities related to $p_i$ become positive as well. At $t = \tau_0$ , the adjusted fraction of consumers jumps from $p_{ct-}^a = a_s = 1$ to $p_{c\tau_0}^a = \sum_{j\in\{s,e,i,r\}} p_{j\tau_0}a_j$ .

Equilibrium is then given by

**Proposition 2.1.** *Consider the BDRA-SEIRD-SIP-LIFT model. The equilibrium stochastic*

[1]Subgroups of populations can have difference discounts for consumption, reflecting their economic status or their health status. The variable $p_c^a$ is adjusted as needed to capture these effects.

*discount factor (SDF) is*

$$\xi_t = \sum_{k=1}^{K} e^{-\beta t} \left(\frac{C_t}{p^a_{ct}}\right)^{-R_k} P_{kt}. \tag{2.14}$$

*where* $\xi_0 = 1$ *. The equilibrium interest rate and market prices of risk are*

$$\begin{aligned} r_t =& \beta + \left(\sum_{k=1}^{K} R_k q_{kt}\right)\left(\hat{\mu}^C_{ot} + \left(\widehat{A}^C_t \frac{\mu^{p^e_w}(t, s^e_{t-})}{p^e_{wt}} - \frac{\mu^{p^a_c}(t, s^e_{t-})}{p^a_{ct}}\right) 1_{\mathcal{E}_t}\right) \\ & - \frac{1}{2}\left(\sum_{k=1}^{K} R_k(1+R_k) q_{kt}\right)(\sigma^C)^2 - \sum_{k=1}^{K} \mu^P_{kt} q_{kt} + \sum_{k=1}^{K} R_k q_{kt}(\mu^C_k - \hat{\mu}^C_t) + \Lambda^e_{12}\theta^J_{t-} \end{aligned} \tag{2.15}$$

$$\theta^C_t = \left(\sum_{k=1}^{K} R_k q_{kt}\right)\sigma^C - \sum_{k=1}^{K} q_{kt}\Delta^C_{kt}, \qquad \theta^G_t = -\sum_{k=1}^{K} q_{kt}\Delta^G_{kt} \tag{2.16}$$

$$\theta^Y_t = -\sum_{k=1}^{K} q_{kt}\Delta^Y_{kt}, \qquad \theta^J_{t-} = \sum_{k=1}^{K} \frac{e^{-\beta t}(C_t)^{-R_k} P_{kt}}{\sum_{k=1}^{K} e^{-\beta t}(C_t)^{-R_k} P_{kt}} \left(1 - (p^a_{ct})^{R_k}\right) \tag{2.17}$$

*where* $\mu^{p^a_c}(t, s^e_t)$ *is the drift of the adjusted population of consumers,* $\hat{\mu}^C_{ot} = \sum_k P_{kt}\mu^C_{ok}$ *is the expected value of the first component of the consumption growth rate,* $\widehat{A}^C_t = \sum_{k=1}^{K} P_{kt} A^C_k$ *is the expected value of* $A^C(s^m)$ *,* $q_{kt} = \frac{P_{kt}(C_t/p^a_{ct})^{-R_k}}{\sum_k P_{kt}(C_t/p^a_{ct})^{-R_k}}$ *is the equilibrium pricing measure, and* $\theta^J_{t-}$ *is the market price of jump risk. The interest rate has a jump premium component* $\theta^J_{t-}\Lambda_{12}$ *.*

**Remark 2.2.** *The SDF is marginal utility evaluated at the equilibrium consumption allocation. Note that it is discontinuous: it jumps down at* $\tau_0$ *, and the relative jump size, i.e., the negative of the market price of jump risk, is*

$$\frac{\Delta\xi_{\tau_0}}{\xi_{\tau_0-}} = \frac{\sum_{k=1}^{K} C^{-R_k}_{\tau_0} P_{k\tau_0}\left(\left(p^a_{c\tau_0}\right)^{R_k} - 1\right)}{\sum_{k=1}^{K} C^{-R_k}_{\tau_0} P_{k\tau_0}} < 0. \tag{2.18}$$

*where* $p^a_{c\tau_0} = 1 + \Delta_i(\lambda_i + \lambda_s a_i - 1)$ *and* $\Delta_i$ *is the size of the jump in* $p_i$ *at* $\tau_0$ *. Coefficient* $\lambda_s = (1-\lambda)(1-\lambda_w)$ *is the fraction of symptomatic mild in the infectious population, while*

$\lambda_i = (1-\lambda)\lambda_w$ *is the fraction of asymptomatic. The expected relative jump is*

$$E_{\tau_0-}\left[\frac{\Delta\xi_{\tau_0}}{\xi_{\tau_0-}}\right] = \frac{\sum_{k=1}^{K} C_{\tau_0}^{-R_k} P_{k\tau_0}\left(\left(p^a_{c\tau_0}\right)^{R_k} - 1\right)}{\sum_{k=1}^{K} C_{\tau_0}^{-R_k} P_{k\tau_0}} \Lambda^e_{12} dt < 0. \tag{2.19}$$

.

The epidemic impact on the SDF is through $p^a_{ct}$ , the adjusted consuming population. A decrease in the fraction of consumers increases consumption per head, hence reduces the SDF. There are three effects on equilibrium coefficients. The first, encapsulated in the term $\hat{A}^C_t \mu^{p^e_w}_t / p^e_w - \mu^{p^a_c}_t / p^a_c$ , is structural in nature. It represents the net impact on the expected output growth rate and the growth rate of the consuming population. The second, arises through the adjusted probabilities $q_{kt}$ which depend on $c_{jt}/a_j = C_t/p^a_{ct}$ . The third arises through the jump associated with the initial infection event. Variations in the adjusted consuming population $p^a_{ct}$ combine with consumption fluctuations to determine their behavior over time. The interest rate level and evolution reflect all effects. Market prices of risk reflect the second and third effects.

The next proposition extends the stock valuation formula in Berrada, Detemple and Rindisbacher (2018) to the epidemic context.

**Proposition 2.3.** *Define the matrix* $\Upsilon(t, s^e_t)$ *as in Proposition 5.1 in the Appendix and suppose that its elements* $\Upsilon_{ij}(t, s^e_t)$ *are finite for all pairs* $(i, j)$ *. The stock price is then given by*

$$S_t = \mathsf{E}_t\left[\int_t^\infty \xi_{t,s} D_s ds\right] = D_t Z_t' \Upsilon(t, s^e_t) P_t \tag{2.20}$$

*where* $\mathsf{E}_t[\cdot]$ *is the conditional expectation and* $Z_t = q_{kt}/P_{kt}$ *is the density of the probability measure* $q$ *with respect to* $P$ *. The stock market return volatility is* $\sigma^S_t = \sqrt{(\sigma^{SC}_t)^2 + (\sigma^{SG}_t)^2 + (\sigma^{SY}_t)^2}$

*where*

$$\begin{bmatrix} \sigma_t^{SC} \\ \sigma_t^{SG} \\ \sigma_t^{SY} \end{bmatrix} = \begin{bmatrix} \rho\sigma^D + \sigma_t^{SCR} + \sigma_t^{SCG} \\ \sqrt{1-\rho^2}\sigma^D + \sigma_t^{SGG} \\ \sigma_t^{SYG} \end{bmatrix} \tag{2.21}$$

*and, using* $diag_K(v)$ *for the diagonal* $K \times K$ *matrix with vector* $v$ *on the diagonal,*

$$\sigma_t^{SCR} = Z_t' diag_K[-R_k\sigma^C] \left( \frac{\Upsilon(t, s_{t-}^e)}{Z_t'\Upsilon(t, s_{t-}^e)p_t} - I_K \right) p_t, \tag{2.22}$$

$$\sigma_t^{S\alpha G} = Z_t' \left( \frac{\Upsilon(t, s_{t-}^e)}{Z_t'\Upsilon(t, s_{t-}^e)p_t} - I_K \right) \text{diag}\left[\Delta_{kt}^{\alpha}\right] p_t, \qquad \alpha \in \{C, G, Y\}. \tag{2.23}$$

The component $\sigma_t^{SCR}$ is the volatility due to consumption uncertainty, and $\sigma_t^{SCG}, \sigma_t^{SGG}, \sigma_t^{SYG}$ are the volatility components associated with beliefs uncertainty. The correlation between the stock return and the consumption growth rate (resp. orthogonalized dividend growth rate) is $\rho_t^{SC} = \sigma_t^{SC}/\sigma_t^S$ (resp. $\rho_t^{SD} = \sigma_t^{SD}/\sigma_t^S$ ). Correlations are stochastic.

**Remark 2.4.** *Note that the stock price, its volatility coefficients, and the market price of jump risk are discontinuous. They jump when the pandemic regime materializes. In contrast, market prices of diffusion risks are independent of the pandemic state variable* $s_t^e$ *. The equity premium, as the product of market prices of risk and volatility components, is discontinuous as well.*

**Remark 2.5.** *If* $s_t = e_1$ *, i.e,. if the pandemic has not yet been triggered, then the price has the additive decomposition,*

$$S_t = D_t Z_t' \Upsilon_1^o P_t + D_t \Lambda_{12}^e Z_t' \Upsilon_1^e(t) P_t. \tag{2.24}$$

*where the first component,* $D_t Z_t' \Upsilon_1^o P_t$ *, corresponds to the price if the pandemic never occurs and* $D_t \Lambda_{12}^e Z_t' \Upsilon_1^e(t) D_t$ *is the pandemic premium, i.e., the present value of the gains in the event a pandemic occurs. The pandemic premium is proportional to the switching intensity* $\Lambda_{12}^e$ *and the dividend level* $D_t$ *. The same additive decomposition holds for volatility coefficients, replacing*

$\Upsilon$ *by* $\Upsilon_1^o$ *and* $\Lambda_{12}^e \Upsilon_1^e(t)$ *, respectively. These expressions follow because* $\Upsilon = \Upsilon_1^o + \Lambda_{12}^e \Upsilon_1^e(t)$ *where, for* $\alpha \in \{o, e\}$ *,* $\Upsilon_1^\alpha$ *is generated by* $G_1^\alpha$ *(see (5.6)-(5.8) for details).*

## 3. Empirical Results

We proceed in two stages. First we estimate the model without pandemic effects, based on pre-pandemic data. Second, we estimate pandemic-related parameters, using data during the COVID-19 outbreak.

## 3.1. Estimating the BDRA Model: Before the Pandemic

The estimation for the BDRA(K,K) model without pandemic effects follows the approach in BDR (2018). Estimation is based on longer time series with 5 additional years of data.

### 3.1.1. Data Description

The estimation is based on quarterly data from January 1957 to December 2019. The per capita consumptions of nondurable goods ( $C_{n,t}$ ) and services ( $C_{s,t}$ ) are obtained from the Saint-Louis Federal Reserve Bank. Consumption growth is defined as

$$\ln \frac{C_{s,t+1} + C_{n,t+1}}{C_{s,t} + C_{n,t}}, \tag{3.1}$$

Other time series are constructed as in Beeler and Campbell (2012). Using the CRSP value weighted return indexes including dividends ( $\text{vwretd}_t$ ) and excluding dividends ( $\text{vwretx}_t$ ) gives the dividend series $D_t$ ,

$$P_{t+1} = P_t \left(1 + \text{vwretx}_{t+1}\right), \qquad D_{t+1} = P_{t+1} \left[\frac{1 + \text{vwretd}_{t+1}}{1 + \text{vwretx}_{t+1}} - 1\right]. \tag{3.2}$$

The price-dividend ratio (PDR) is obtained by dividing the current price index level by the sum of the 12 previous months' dividends. All further computations and estimations use the

log of the PDR. Quarterly returns are constructed from log monthly returns. Real returns are obtained by adjusting for inflation using the seasonally adjusted consumer price index (obtained from the Saint-Louis Federal Reserve Bank). Quarterly series of ex-ante real three-month rates and real ten-year rates are constructed from monthly series of nominal yields as in Beeler and Campbell (2012). The ex-post real rate is obtained by subtracting the realized inflation from the observed three-month treasury bill rate. It is then regressed against the average quarterly log inflation over the previous year $\pi_{t-12,t}$ (annual log inflation divided by four) and the three-month nominal yield $y_{3,t}$ ,

$$y_{3,t} - \pi_{t,t+3} = \beta_0 + \beta_1 y_{3,t} + \beta_2 \pi_{t-12,t} + \varepsilon_{t+3}. \tag{3.3}$$

The ex-ante real rate is then defined as $\hat{\beta}_0 + \hat{\beta}_1 y_{3,t} + \hat{\beta}_2 \pi_{t-12,t}$ . The same procedure is used, with an adjustment for the time period, for the ten-year ex-ante real rate. [2]

The information variable in Eq. (2.10) is defined as the unemployment rate (UE)

$$I_t = UE_t,$$

The data for UE is obtained from the Saint-Louis Federal Reserve Bank.

### 3.1.2. Estimation Procedure

Model parameters are estimated using a just identified sequential GMM procedure pioneered by Ogaki (1993). The set of parameters is partitioned into subsets $\Theta = \Theta_1 \cup \Theta_2 \cup \Theta_3$ with

$$\Theta_1 \equiv \left\{\sigma^C, \sigma^D, \sigma^I, \rho, \rho^{IC}, \rho^{ID}\right\},$$
$$\Theta_2 \equiv \left\{\mu_1^C, \mu_2^C, \mu_3^C, \mu_1^D, \mu_2^D, \mu_3^D, \mu_1^I, \mu_2^I, \mu_3^I, \lambda_{12}, \lambda_{13}, \lambda_{21}, \lambda_{23}, \lambda_{31}, \lambda_{32}, R_{\min}, \beta\right\},$$
$$\Theta_3 \equiv \{R_2, R_3\}.$$

[2] This procedure is also used by Harvey (1988) to test whether the real term premium can forecast recessions.

The first subset, $\Theta_1$ , contains parameters of the covariance matrix of consumption, dividends and the information variable (unemployment). Parameter estimates are obtained by matching corresponding sample moments. Given the constant volatility structure of state variables these estimates are equivalent to maximum likelihood estimates (MLE).

The second subset, $\Theta_2$ , determines the steady state behavior of the model. These parameters are estimated using sample analogs of the invariant theoretical counterparts.

Parameters in the third subset, $\Theta_3$ , do not affect the steady state equilibrium values, but only the dynamics of equilibrium quantities. In order to address this part of the estimation procedure, we rely on the extensive literature originating from Campbell and Shiller (1988) that identifies a link between stock returns and PDR. We consider the following two moment conditions (i) correlation between log simple returns and changes in log PDR, and (ii) correlation between log simple returns and changes in log PDR lagged by one quarter. Given the estimates for parameters in the subset $\Theta_1 \cup \Theta_2$ , these two moments within the model use filtered values of state variables to generate a sample path that depends on the unknown parameters in $\Theta_3$ . Parameters in $\Theta_3$ are estimated by minimizing the squared error of deviations of these two moments of sample paths within the model and in the sample.

Table 1 summarizes the moment conditions used in the estimation of the different sets of parameters. Additional details and justification of this procedure can be found in BDR (2018).

### 3.1.3. Parameter Estimates and Model Performance

Table 2 shows that parameter estimates are close to their empirical values, and typically lie within the 95% confidence bands or are close to the edges of these bands. Exceptions are the mean 3-month and 10-year yields and the volatility of the 10-year yield. Relative to the estimation results in BDR (2018), which is based on the shorter sample from 1957 to 2014, the mean consumption growth rate is further away from its sample value.

Table 3 reports estimates for the drifts of consumption, unemployment, and dividends, and for the preference parameters, in the three growth regimes. Patterns for the coefficients per-

taining to consumption and unemployment are the same as in BDR (2018), with reduction in some of the point values obtained. In contrast, dividend drift coefficients display an increasing pattern, as opposed to the previous U-shape pattern, due to an increase in the estimate for regime 2. The risk aversion function implied by estimates of preference parameters displays the same inverted U-shape as in BDR (2018), but with a slight upward shift. Hence, the interpretation of regime 2 as a recession regime is also maintained, even though the estimation did not impose a priori restrictions on the ordering of regimes. Finally, standard deviation estimates for consumption, dividend and unemployment are about the same, whereas the correlations between dividend and consumption (positive), and dividend and unemployment (negative) are both cut in half.

Overall, the results obtained based on the augmented sample 1957-2019 are consistent with those in BDR (2018) for the period 1957-2014.

Table 1: Moment conditions. The table lists the moment conditions used for the just identified sequential GMM estimation of model parameters. Theoretical expressions for steady state values are in Detemple et al (2018). Sample moments are based on standard sample statistics for means, standard deviations, correlation, and auto-correlation coefficients. The operator $\widehat{CORR}_{T,\Theta_3}[X_t, Y_t]$ calculates the empirical correlation coefficient between $X_t$ and $Y_t$ based on model trajectories of length $T$ as a function of parameters $\Theta_3$ .

| Parameter estimation: moment conditions | | |
|---|---|---|
| Moment condition | Invariant moment (definition) | Sample moments |
| Covariance of state variables: $\Theta_1 = \left\{\sigma^C, \sigma^D, \sigma^I, \rho, \rho^{IC}, \rho^{ID}\right\}$ | | |
| 1. Vol. cons. | $\sigma^C$ | $\widehat{STD}_T[\Delta \log C_t]$ |
| 2. Vol. div. | $\sigma^D$ | $\widehat{STD}_T[\Delta \log D_t]$ |
| 3. Vol. unemp. | $\sigma^I$ | $\widehat{STD}_T[\Delta \log I_t]$ |
| 4. Corr. cons., div. | $\rho$ | $\widehat{CORR}_T[\Delta \log C_t, \Delta \log D_t]$ |
| 5. Corr. cons., unemp. | $\rho^{IC}$ | $\widehat{CORR}_T[\Delta \log C_t, \Delta \log I_t]$ |
| 6. Corr. div., unemp. | $\rho^{ID}$ | $\widehat{CORR}_T[\Delta \log D_t, \Delta \log I_t]$ |
| Steady state values: $\Theta_2 = \left\{\mu_1^C, \mu_2^C, \mu_3^C, \mu_1^D, \mu_2^D, \mu_3^D, \mu_1^I, \mu_2^I, \mu_3^I, \lambda_{12}, \lambda_{13}, \lambda_{21}, \lambda_{23}, \lambda_{31}, \lambda_{32}, R_{\min}, \beta\right\}$ | | |
| 1. Exp. cons. | $\mu_\infty^C + 0.5\left(\sigma^C\right)^2$ | $\widehat{E}_T[\Delta \log C_t]$ |
| 2. Exp. div. | $\mu_\infty^D + 0.5\left(\sigma^D\right)^2$ | $\widehat{E}_T[\Delta \log D_t]$ |
| 3. Exp. unemp. | $\mu_\infty^I + 0.5\left(\sigma^I\right)^2$ | $\widehat{E}_T[\Delta \log I_t]$ |
| 4. Log-PDR | $\log \frac{S_\infty}{D_\infty}$ | $\widehat{E}_T[\log PDR_t]$ |
| 5. Exp. 3-m. yield | $Y_\infty^{\infty+0.25}$ $\tau = 0.25$ | $\widehat{E}_T\left[Y_t^{t+0.25}\right]$ |
| 6. Exp. 10-y. yield | $Y_\infty^{\infty+10}$ $\tau = 10$ | $\widehat{E}_T\left[Y_t^{t+10}\right]$ |
| 7. Stock volatility | $\sigma_\infty^S$ | $\widehat{STD}[\Delta \log S_t]$ |
| 8. Volatility of 10-y. yield | $\sigma_\infty^Y(\tau)$ | $\widehat{E}_T\left[Y_t^{t+0.25}\right]$ |
| 9. Exp. excess return | $\mu_\infty^S - r_\infty$ | $\widehat{E}_T[\Delta \log S_t - r_t]$ |
| 10. Corr. return, cons. | $\rho_\infty^{S,C}$ | $\widehat{CORR}_T[\Delta \log S_t, \Delta \log C_t]$ |
| 11. Corr. return, div. | $\rho_\infty^{S,D}$ | $\widehat{CORR}_T[\Delta \log S_t, \Delta \log D_t]$ |
| 12. Corr. 3-m. yield, cons. | $\rho_\infty^{Y,C}(\tau)$ $\tau = 0.25$ | $\widehat{CORR}_T\left[Y_t^{t+0.25}, \Delta \log C_t\right]$ |
| 13. Corr. 3-m. yield, div. | $\rho_\infty^{Y,D}(\tau)$ $\tau = 0.25$ | $\widehat{CORR}_T\left[Y_t^{t+0.25}, \Delta \log D_t\right]$ |
| 14. Corr. 10-y. yield, cons. | $\rho_\infty^{Y,C}(\tau)$ $\tau = 10$ | $\widehat{CORR}_T\left[Y_t^{t+10}, \Delta \log C_t\right]$ |
| 15. Corr. 10-y. yield, div. | $\rho_\infty^{Y,D}(\tau)$ $\tau = 10$ | $\widehat{CORR}_T\left[Y_t^{t+10}, \Delta \log D_t\right]$ |
| 16. Volatility log-PDR ratio | $\sigma_\infty^{\log-\mathrm{PDR}}$ | $\widehat{STD}_T[\log PDR_t]$ |
| 17. Corr. log-PDR, cons. | $\rho_\infty^{\log-\mathrm{PDR},C}$ | $\widehat{CORR}_T[\log PDR_t, \Delta \log C_t]$ |
| Path dynamics: $\Theta_3 = \{R_2, R_3\}$ | | |
| 1. Corr. log-PDR, return | $\widehat{CORR}_{T,\Theta_3}[\Delta \log \mathrm{PDR}_t, \Delta logS_t]$ | $\widehat{CORR}_T[\Delta \log \mathrm{PDR}_t, \Delta logS_t]$ |
| 2. Corr. log-PDR, return (1 lag) | $\widehat{CORR}_{T,\Theta_3}[\Delta \log \mathrm{PDR}_{t-1}, \Delta logS_t]$ | $\widehat{CORR}_T[\Delta \log \mathrm{PDR}_{t-1}, \Delta logS_t]$ |

Table 2: Moment conditions and confidence intervals. Model moment conditions are based on stationary values and estimated parameters. Confidence bounds are obtained using the stationary bootstrap for weakly dependent data of Politis and Romano (1994). The 95% confidence intervals are based on 1000 replications and optimal average blocksize.

| | Model | Data | Confidence lower bound | Confidence upper bound |
|---|---|---|---|---|
| | | Mean | | |
| Consumption growth | 0.01336 | 0.01878 | 0.01619 | 0.02094 |
| Dividend growth | 0.00862 | 0.02089 | 0.00842 | 0.03150 |
| Unemployment growth | 0.00586 | 0.00492 | -0.03042 | 0.02911 |
| Log PDR | 3.77885 | 3.61139 | 3.56689 | 3.66143 |
| Excess returns | 0.05318 | 0.05238 | 0.00914 | 0.09553 |
| Mean 10-year yield | 0.02919 | 0.02187 | 0.02083 | 0.02299 |
| Mean 3-month yield | 0.02968 | 0.00864 | 0.00691 | 0.01048 |
| | | Volatility | | |
| Log PDR | 0.16681 | 0.17046 | 0.15448 | 0.19169 |
| Excess returns | 0.21168 | 0.16792 | 0.14972 | 0.19018 |
| 10-year yield | 0.02101 | 0.00902 | 0.00828 | 0.01004 |
| | | Correlations | | |
| Stock returns / consumption | 0.08920 | 0.24046 | 0.11367 | 0.36834 |
| Stock returns / dividend | 0.26655 | 0.09437 | –0.04243 | 0.20755 |
| 10-year yield / consumption | 0.12260 | 0.14894 | 0.00985 | 0.27520 |
| 10-year yield / dividend | -0.04092 | -0.17219 | -0.27332 | -0.06401 |
| 3-month yield / consumption | 0.26685 | 0.25407 | 0.13769 | 0.36103 |
| 3-month yield / dividend | -0.02821 | -0.08680 | -0.20495 | 0.04073 |
| log PDR / consumption | 0.26323 | 0.22340 | 0.08522 | 0.35540 |
| | | Stock return and log(PDR) correlation | | |
| Contemporaneous | 0.99716 | 0.96457 | 0.9402 | 0.9758 |
| Lagged log(PDR) | 0.06060 | 0.06030 | -0.0707 | 0.2064 |

Table 3: Estimated parameters (standard errors). GMM parameter estimates with standard errors obtained from stationary bootstrap (Politis and Romano (1994)).

| Growth regime | | | Growth regime | | |
|---|---|---|---|---|---|
| Normal | Low | High | Normal | Low | High |
| Consumption | | | Unemployment | | |
| $\mu_1^C$ | $\mu_2^C$ | $\mu_3^C$ | $\mu_1^{UE}$ | $\mu_2^{UE}$ | $\mu_3^{UE}$ |
| 0.00969 | 0.00572 | 0.03554 | -0.00067 | 0.12653 | –0.09982 |
| (0.0081) | (0.0075) | (0.0102) | (0.0332) | (0.0460) | (0.0424) |
| Dividend | | | Preferences: risk aversion | | |
| $\mu_1^D$ | $\mu_2^D$ | $\mu_3^D$ | $R_1$ | $R_2$ | $R_3$ |
| 0.00672 | 0.00746 | 0.01707 | 2.06340 | 2.5550 | 2.2416 |
| (0.0099) | (0.0098) | (0.0104) | (0.3788) | (0.0983) | (0.0133) |

| Preferences: subjective discount rate | | |
|---|---|---|
| $\beta_1$ | $\beta_2$ | $\beta_3$ |
| 0.01000 | 0.01000 | 0.01000 |
| (0.0021) | (0.0021) | (0.0021) |

Standard deviations and correlations

| | Consumption | Dividend | Unemployment |
|---|---|---|---|
| Consumption | 0.0092 | 0.0799 | –0.3626 |
| | (0.0641) | (0.1096) | (0.2230) |
| Dividend | 0.0799 | 0.0449 | –0.1836 |
| | (0.1096) | (0.0744) | (0.1895) |
| Unemployment | –0.3626 | –0.1836 | 0.1214 |
| | (0.2230) | (0.0.1895) | (0.9587) |

Infinitesimal generator

| | Normal | Low | High | Steady state probabilities |
|---|---|---|---|---|
| Normal | –0.07343 | 0.07343 | 3.859425 E-07 | 0.645 |
| | - | (0.0148) | (1.86 E-06) | |
| Low | 0.24417 | –0.25736 | 0.01320 | 0.184 |
| | ( 0.0343) | - | (0.0037) | |
| High | 0.01426 | 1.789710 E-07 | –0.01426 | 0.170 |
| | (0.0046222) | (1.70 E-06) | - | |

## 3.2. Estimating the BDRA Model: During the Pandemic

We now focus on the pandemic period, assuming that risk aversion parameters do not depend on the pandemic regime, $R_k(s_t^e) = R_k$ and parameters $A^C(s_t^m) = A^C, A^G(s_t^m) = A^G$ are constants across economic regimes. First, we complete the SIP-LIFT model by specifying the transmission intensity. Second, we describe the estimation procedure for the pandemic-related parameters. Last, we present the results and discuss performance.

### 3.2.1. Transmission Intensity Specification

We consider a version of the SIP-LIFT model with time-decay and threshold effects in the transmission intensity $\beta$. We assume

$$\beta_t = \beta_0 e^{-\kappa_0 t} 1_{t \leqslant t_1} + \beta_1 e^{\kappa_1 (t - t_m)} 1_{t_1 < t \leqslant t_2} + \beta_2 e^{-\kappa_2 (t - t_2)} 1_{t_2 < t} \tag{3.4}$$

where $t_1, t_2$ are transmission intensity change dates, $\kappa_0, \kappa_2$ are decay rates respectively prevailing up to the first date and after the second one, and $\kappa_1$ is an expansion rate in the intermediate period up to time $t_2$. The parameter $\beta_1 = \beta_0 e^{-\kappa_0 t_1}$ is the value at $t_1$ and $\beta_2 = \beta_1 e^{-\kappa_1 (t_2 - t_m)}$ at $t_2$. The parameter $t_m \in [t_1, t_2]$ cuts the intermediate period in two parts. From $t_1$ to $t_m$ the transmission intensity decreases, from $t_m$ to $t_2$ it increases. This formulation captures social distancing effects taking place as the epidemic propagates and disease mitigation recommendations by health authorities and governmental agencies. For instance, the dates $t_1, t_2$ might be associated with recommendations to implement and lift a SIP policy. The reversal of decay during the period $[t_1, t_2]$ captures weariness and overconfidence effects that may develop during SIP.

### 3.2.2. Estimation Procedure for Pandemic Parameters

In light of Sections 2.1 and 3.2.1, and Appendix A, the set of pandemic propagation parameters is $\Theta_4 = \{p_{i_0}, \beta_0, t_1, t_2, \kappa_0, \kappa_1, \kappa_2, \sigma, \gamma, \mu_i, q, q_2\}$. In addition, we have parameters in

$\Theta_5 = \{A^C, A^G, A^Y(s_t^m), a_i, a_l, \omega, h\}$ governing the impact of the pandemic on the time series of consumption, dividend and unemployment. Hence, the full set of pandemic-related parameters to be estimated is $\Theta_4 \cup \Theta_5$ .

Estimation is based on the number of new COVID-19 cases, the level of the S&P 500 index during the outbreak and a measure of the index return volatility. Data for new cases are from the COVID Tracking Project.[3] Volatility is proxied by the average squared total return on the S&P 500 index computed over a 10 days rolling window. The sample period is January 1 2020 until August 7 2020, therefore covering the first and second waves of the COVID pandemic in the US.[4]

All target quantities are available at daily frequency. Input quantities in the model, however, are available at different frequencies. Unemployment, consumption and dividend are available at monthly frequency and are held constant between observations. This results in innovation processes that are updated at monthly frequency. The regimes conditional probabilities $p_t$ therefore change at monthly frequency. The drift processes of unemployment, consumption and dividend, are adjusted at daily frequency using the pandemic related effect $A_t^{\alpha}(s_t^e)\frac{\mu^{p_w^e}(t,s_t^e)}{p_w^e}1_{\mathcal{E}}$ . The stock price level and volatility are functions of the conditional probabilities, the consumption and dividend level. They also depend on the volatility of the conditional probabilities which are functions of the drift processes of unemployment, consumption and dividend. It follows that through the updating procedure of the drift processes driven by the pandemic model, stock price level and volatility can also be updated at daily frequency. The entire process is displayed in a diagram in Figure 1. The estimation is performed by minimizing the squared distance between model implied and observed (i) stock volatility (ii) stock price level and (iii) number of new COVID cases, all measured at daily frequency.

[3]See https://covidtracking.com/data/us-daily

[4]The quantitative easing program started in March 2020 with a significant inflation of the FED balance sheet. There is strong empirical evidence that QE affected stock prices, but with a significant delay. We focus on the immediate real effect of the pandemic and do not extend the analysis to a period where the market is too heavily biased by QE.

### 3.2.3. Parameter Estimates

The lower panel in Table 2 reports estimates of pandemic propagation and related policy parameters in $\Theta_4$. The initial transmission rate $\beta_0 = 2.3110$ is found to decay at rate $\kappa_0 = 3.8165$ pre-SIP, decay/appreciate at rate $\kappa_1 = 23.4286$ during SIP, to finally decay at rate $\kappa_2 = 13.2838$ post-SIP. Estimates of infection regime changes are respectively $t_1 = 61.5119$ and $t_2 = 120.2494$, roughly in line with average times of SIP and LIFT implementations across states. The pandemic birth time is estimated at $\tau_0 = 18.8987$, and the time marking an acceleration of transmission during SIP is $t_m = 66.4458$. The mean latency duration is $\sigma^{-1} = 12.7294$ days, and the mean infectious duration $\gamma^{-1} = 12.0767$ days. Both values are consistent with estimates reported during the initial phases of the COVID-19 outbreak. The fraction of severe and asymptomatic cases are estimated at $\lambda = 0.0334$ and $(1-\lambda)\lambda_w = 0.5772$, respectively, again consistent with reported values. The disease mortality parameter $\mu_i = 2.22 \times 10^{-5}$ is commensurate with COVID-19 mortality statistics. As might be expected, the natural immunity rate $\nu^o = 4.7 \times 10^{-6}$ is extremely low. Finally, the migration rates into and out of lockdown are respectively $q = 0.080184$ and $q_2 = 0.000849$. Compliance $q$ is low because some states never went into lockdown while others implemented SIP at various dates. In addition, the policy did not apply to essential workers. Reverse migration $q_2$ is even lower because businesses were slow to reopen or because firms continued operating using work-at-home.

The upper panel of Table 2 reports estimates of the economic effects of the pandemic on the drifts of consumption, orthogonal dividend and orthogonal unemployment. The sensitivity of consumption is estimated at $A^C(s_t^e) = 5.2649 \times 10^{-3}$, showing a low response to the propagation via $p_w^e$. The sensitivity of dividend is even lower at $A^C(s_t^e) = 0.8880 \times 10^{-3}$. Estimates of both of these coefficients are positive indicating a negative impact as the growth rate of the working population falls. In contrast the sensitivity of orthogonal unemployment, assumed to depend on the state of the epidemic in the estimation, is negative in all of these states. Its greatest magnitudes are in states $s_t^e = e_1$ and $s_t^e = e_3$ at respectively $A^Y(e_1) = -0.0315006$ and $A^Y(e_3) = -0.6988067$. Unemployment responds strongly to the growth rate of the workforce

pre- and post-pandemic, regimes during which that growth rate does not vary much. At $A^Y(e_2) = -0.0008576$ , the response during the pandemic is weaker because the growth rate exhibits a very strong negative response. The product of the two therefore produces a significant impact during the outbreak. The efficiency of work-at-home is estimated at $\omega = 0.7553$ , and the fraction of individuals working at home is $h = 0.9622$ . The efficiency loss associated with work-at-home can be attributed to frictions in the organization of work, the transmission of information and the implementation of decisions and processes. Last, the consumption discount factors of ill and laid-off individuals are estimated at $a_i = 0.9625$ and $a_l = 0.99999$ , respectively. Individuals stricken by the pandemic shift their consumption basket towards medical goods and services, leading to a small reduction in overall expenditures. Laid-off individuals consume at nearly the same rate during the pandemic due to government subsidies and related support schemes.

### 3.2.4. Model Performance: Targeted Variables

We now examine the performance of the BDRA-SEIRD-SIP-LIFT model relative to variables that were targeted in the estimation procedure, i.e., the number of new COVID-19 cases, the volatility of the S&P 500, and the level of the S&P 500.

Figure 2 shows that the estimated model stays close to the observed number of cases in the data. The most significant deviation occurs toward the end of the wave of the outbreak, between days 140 and 150 counting from January 1, 2020. The match during the second wave, between days 160 and 220, is very close.

Figure 3 demonstrates that the SIP-LIFT model is able to replicate the rapid increase and decrease in volatility that took place during the first wave of the COVID-19 pandemic as well as the magnitude and inverted V-shape of the effect recorded. In comparison the standard BDRA model without pandemic effect, called the base model hereafter, only generates an increase in volatility with a significant delay, and of much smaller amplitude; see Figure 10. It is also unable to reproduce the inverted V-shape of the volatility event. The reason for the discrepancy

between the performances of the two models is because the base model reacts only when the recession probability reaches a peak, whereas the pandemic model reacts immediately following an increase in the number of COVID-19 cases. This discrepancy is examined in more details in Section 3.2.6 below.

Figure 4 establishes that the BDRA-SEIRD-SIP-LIFT model is able to reproduce the behavior of the S&P 500 during the first two waves of the outbreak. The model generates the asymmetric V-shape adjustment of the index and closely matches the trough. It also matches the steep decline of the index, albeit with a short delay and a slight overshoot prior to the decline. Finally, it displays the progressive recovery found in the data, but with more pronounced short term swings.

### 3.2.5. Model Performance: Non-Targeted Variables

Let us now focus on performance relative to non-targeted variables. In a first step we examine the implied unemployment growth rate, consumption growth rate and dividend growth rate. In a second step, we study the local moments of the volatility process.

Figure 5 shows that the model implied growth rate in unemployment matches the data remarkably well. Most significantly, it increases and decreases with a very short lag relative to the data, matches the timing of the peak rate, and picks up the small rebound recorded after the first wave. Values obtained are also close to the data. In contrast, the base model (not displayed) is flat near zero throughout the period examined, hence unable to reproduce any aspect of the evolution of the unemployment growth rate. The pattern recorded in the BDRA-SEIRD-SIP-LIFT model therefore reflects the impact of the coefficient $A^Y(s_t^e)$. In that regard, it is important to remember that the unemployment growth rate was not targeted in the optimization. The targeted quantities in the minimization of errors are the S&P 500 level and volatility and the number of COVID-19 cases.

Figure 6 establishes that the model-implied consumption growth rate closely fits the data as well. It captures the timing and magnitude of the drop during the first wave of the outbreak,

as well as the quick rebound that followed. However, it fails to capture the smaller temporary increase in the consumption growth rate during the second wave.

Figure 7 illustrates the behavior of the model-implied dividend growth rate. The model-implied pattern matches the pattern in the data, albeit with a substantial lead. The reason for this anticipatory behavior is that the dividend series constructed from the data is a a yearly average of dividends paid on stocks in the index, whereas the model-implied counterpart updates at a monthly frequency, hence reacts faster to the propagation of the pandemic.

### 3.2.6. Regime Probabilities and Pandemic Model

To better understand the performance of the BDRA-SEIRD-SIP-LIFT model it is informative to focus on the dynamics of the conditional regime probabilities. Figure 8 and 9 display their evolution for the model with pandemic and the base model. The shaded area corresponds to the brief recession period February through April identified by NBER. The base model overestimates the duration of the recession, and has a major reaction with a delay of two months. The volatility in the base model, illustrated in Figure 10, increases with a delay exceeding two months and stays high for several months thereafter. It therefore completely misses the observed spike in volatility during the first wave of the pandemic. On the contrary, the conditional probabilities in the SIP-LIFT model react sooner and with smaller magnitudes. The increase in the recession probability is confined to the corresponding NBER recession period. The volatility, in the SIP-LIFT model, is directly impacted by the increase in the number of COVID cases through changes in the drift parameters in the consumption, unemployment and dividend dynamics. It follows that it not only generates a high level of volatility at the onset of the crisis, but also is able to capture the rapid decrease as the number of new cases decreases. The introduction of this new channel allows the model to correctly estimate the duration of the recession, and therefore avoids the delayed increase in volatility and extended duration of the volatility event that is observed in the base model.

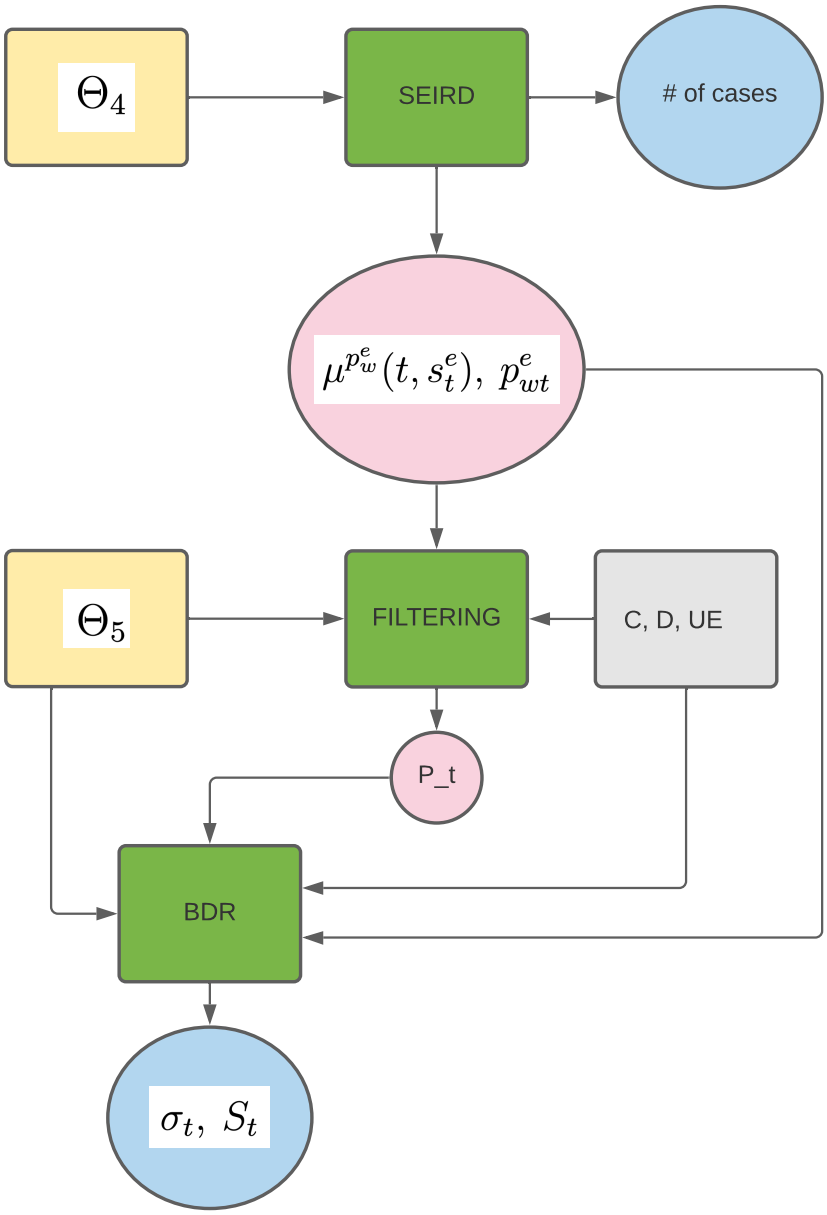


Figure 1: Estimation process diagram. Box colors are Yellow: parameters, Green: models, Grey: data, Pink: model output - intermediary quantities, Blue: model output - target quantities.

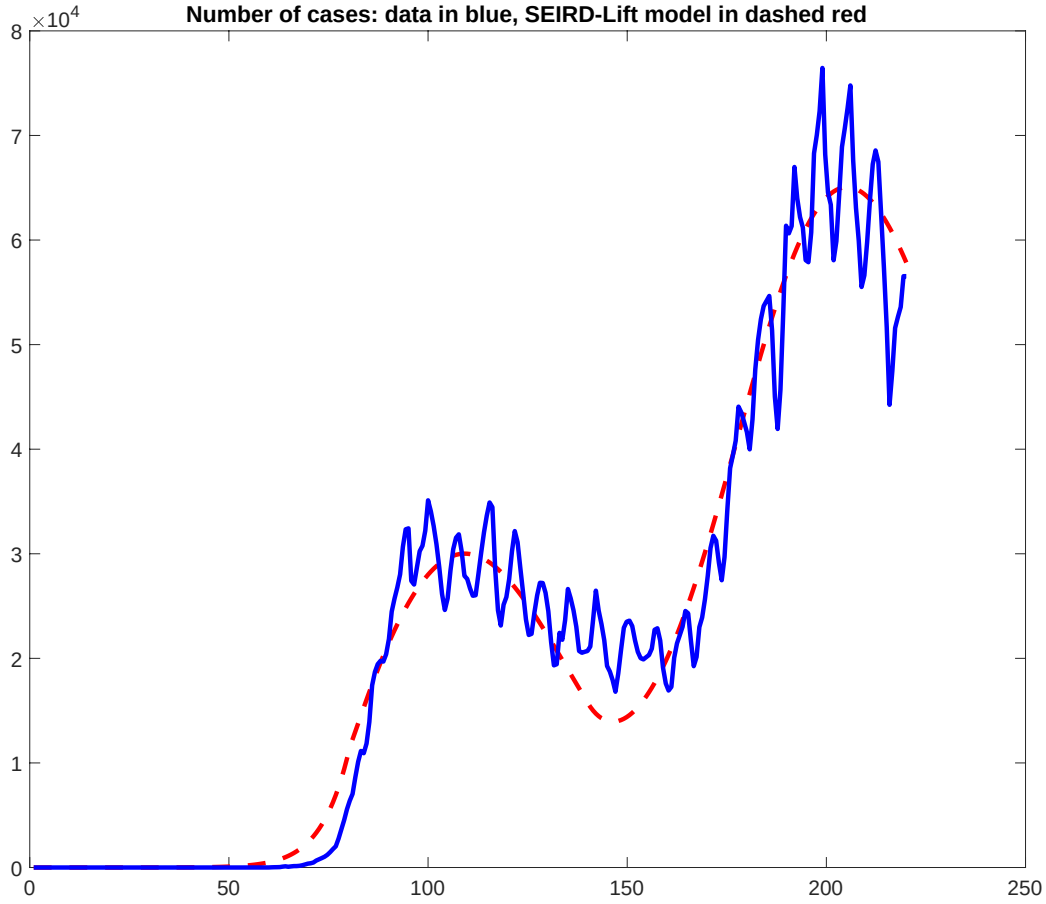


Figure 2: Number of cases in the data (blue) and in the pandemic optimized model (red)

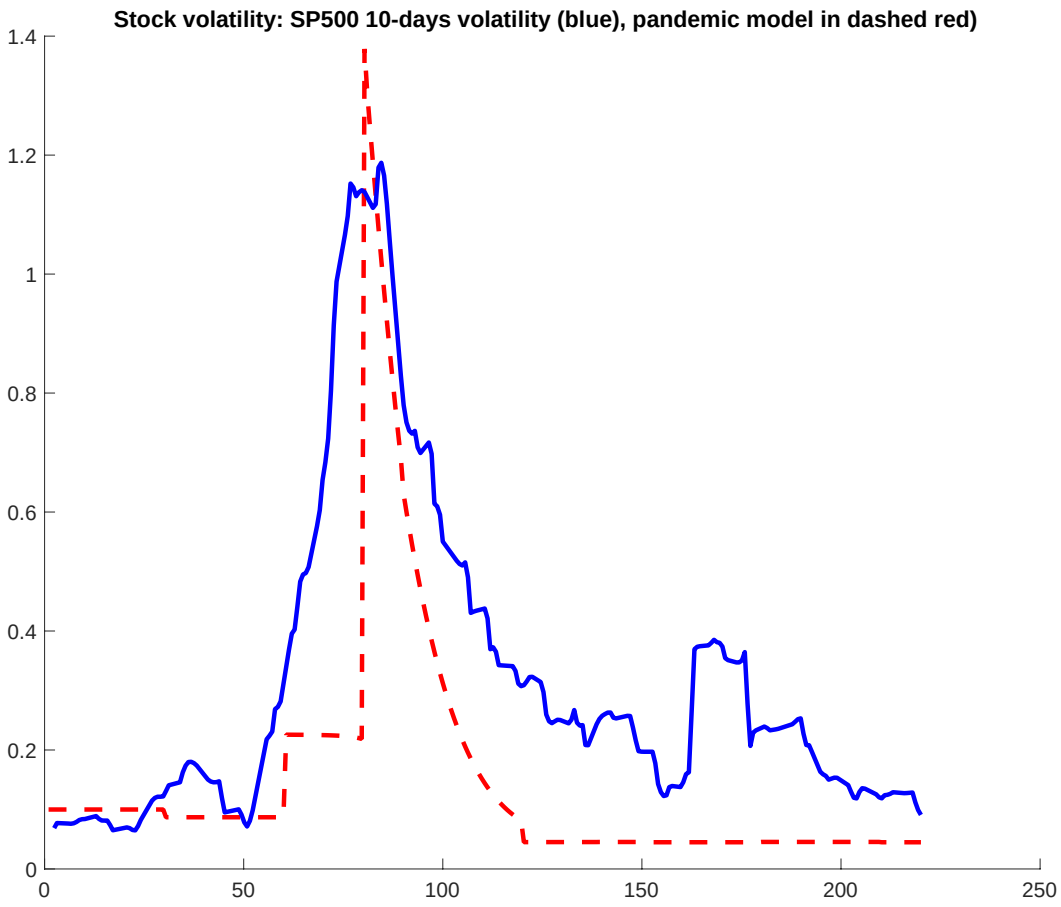


Figure 3: Stock price volatility: 10 days rolling volatility of the SP500 in blue, pandemic model with LIFT in red dashed.

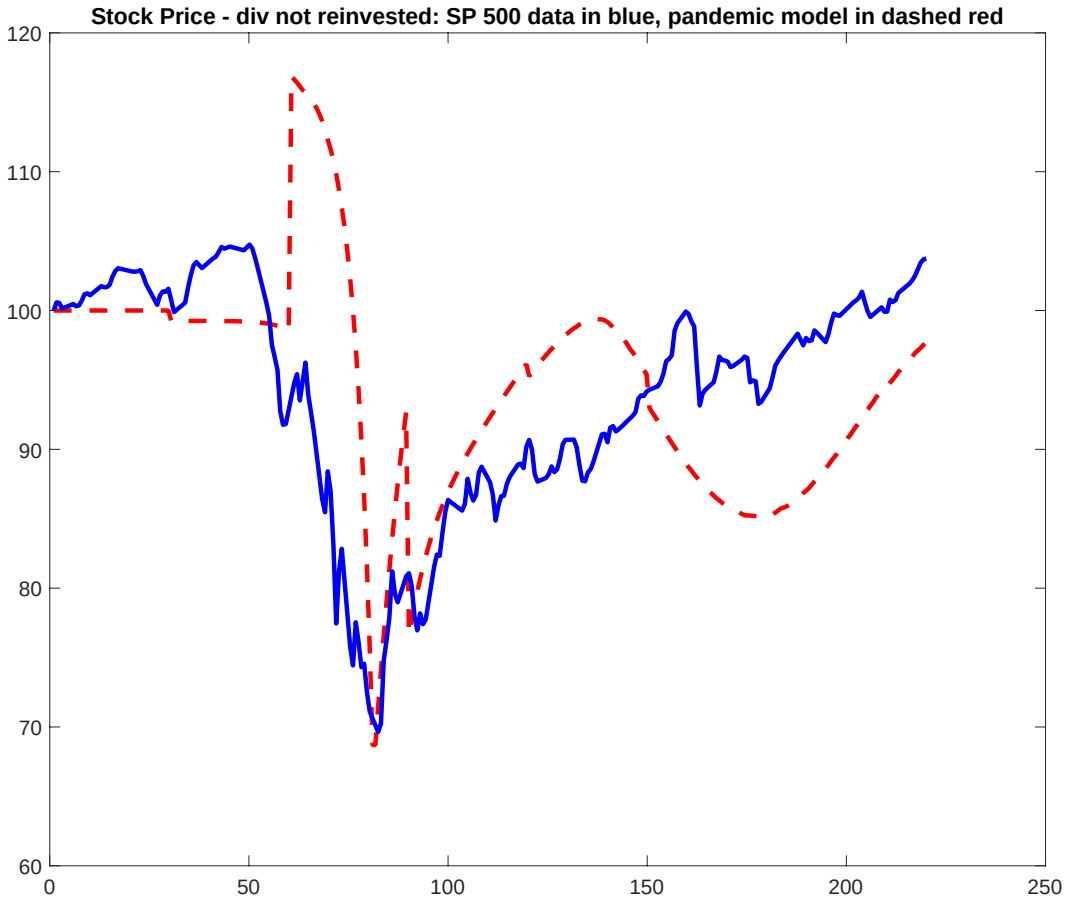


Figure 4: Stock price level: SP500 dividend not reinvested in blue, pandemic model with LIFT in red dashed. Prices are normalized at 100 on January 1st

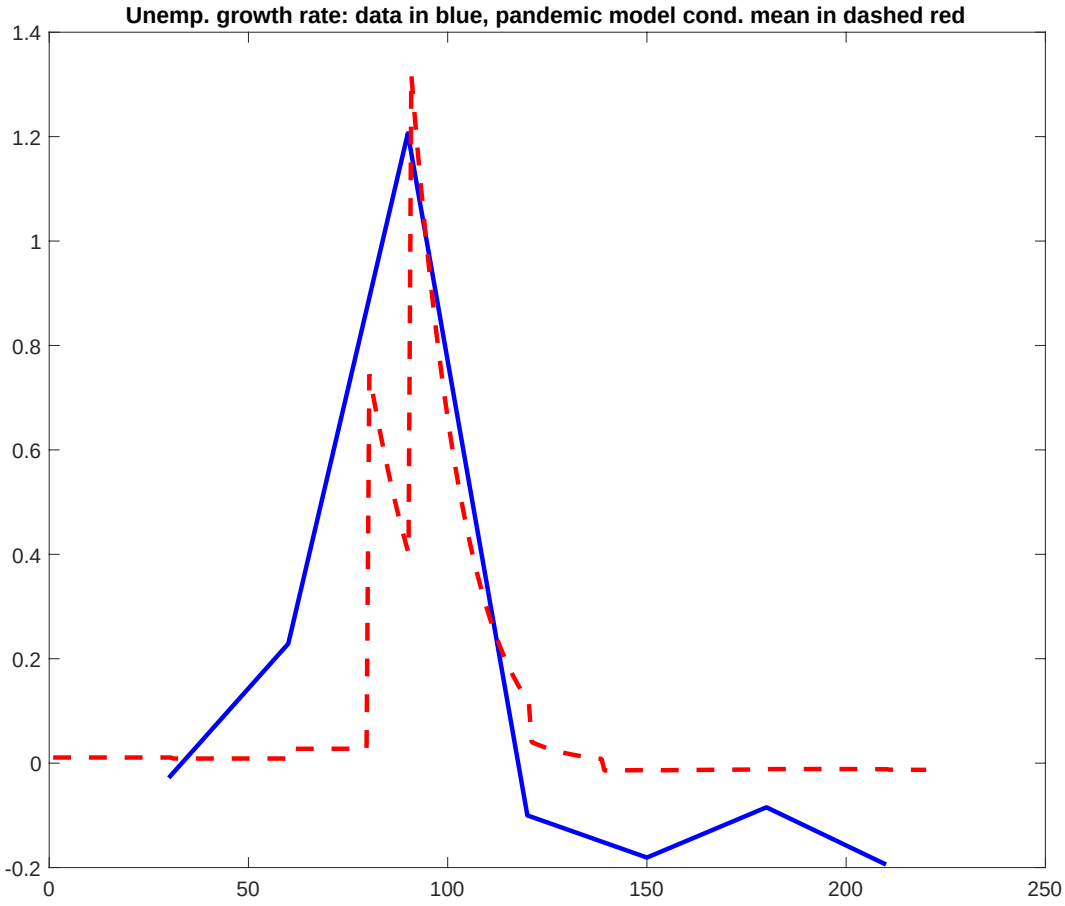


Figure 5: Unemployment growth rate. Monthly data in blue, pandemic model with LIFT in red dashed

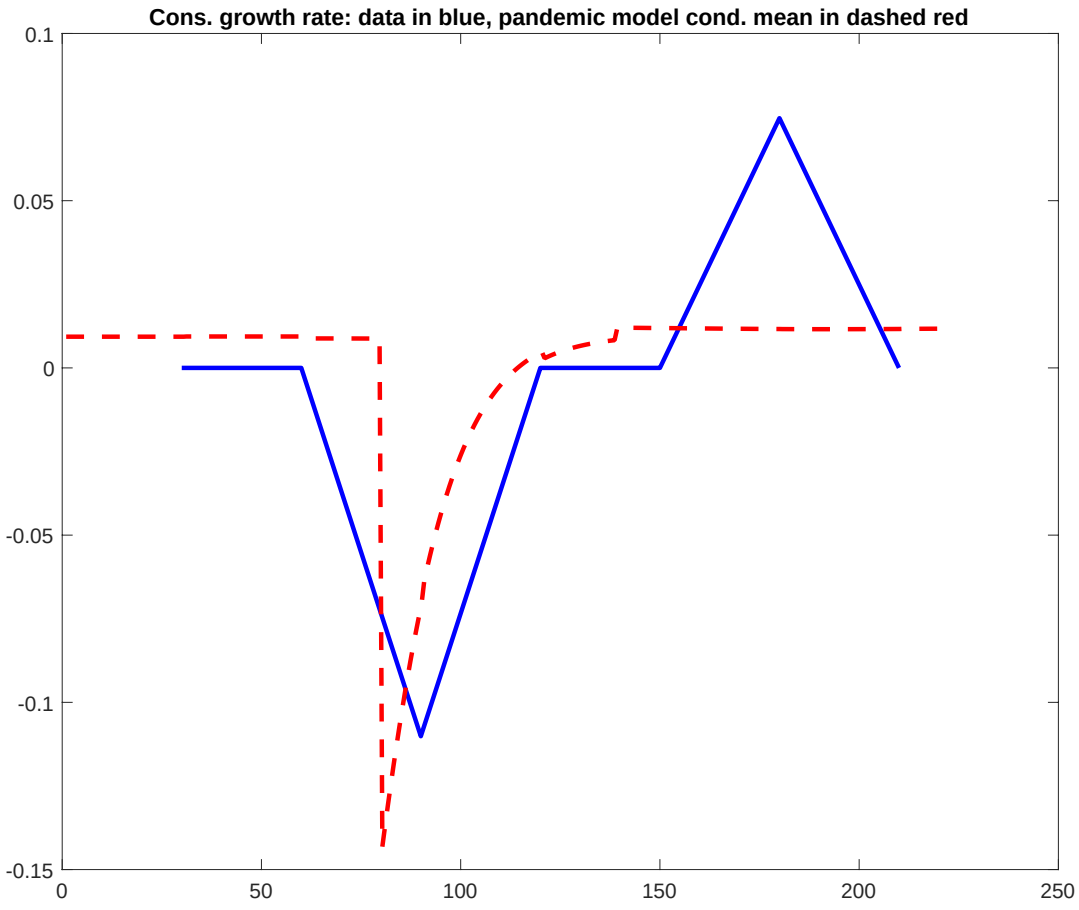


Figure 6: Consumption growth rate. Monthly data in blue, pandemic model with LIFT in red dashed


Figure 7: Dividend growth rate. Monthly data in blue, pandemic model with LIFT in red dashed

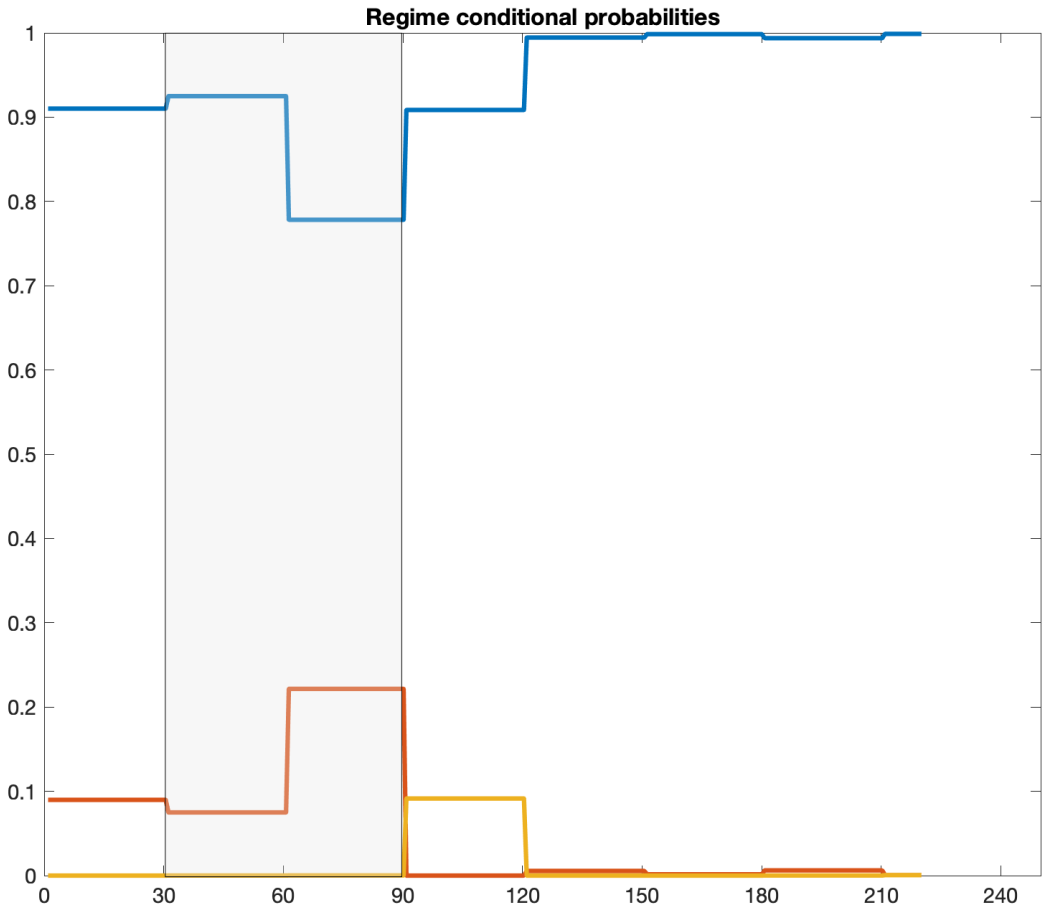


Figure 8: Conditional regime probabilities for the model with pandemic. Normal regime in blue, Recession regime in red, Boom regime in yellow. The shaded area corresponds the NBER recession period. The sample period is January 1st through August 7th. The X-axis displays the day number.

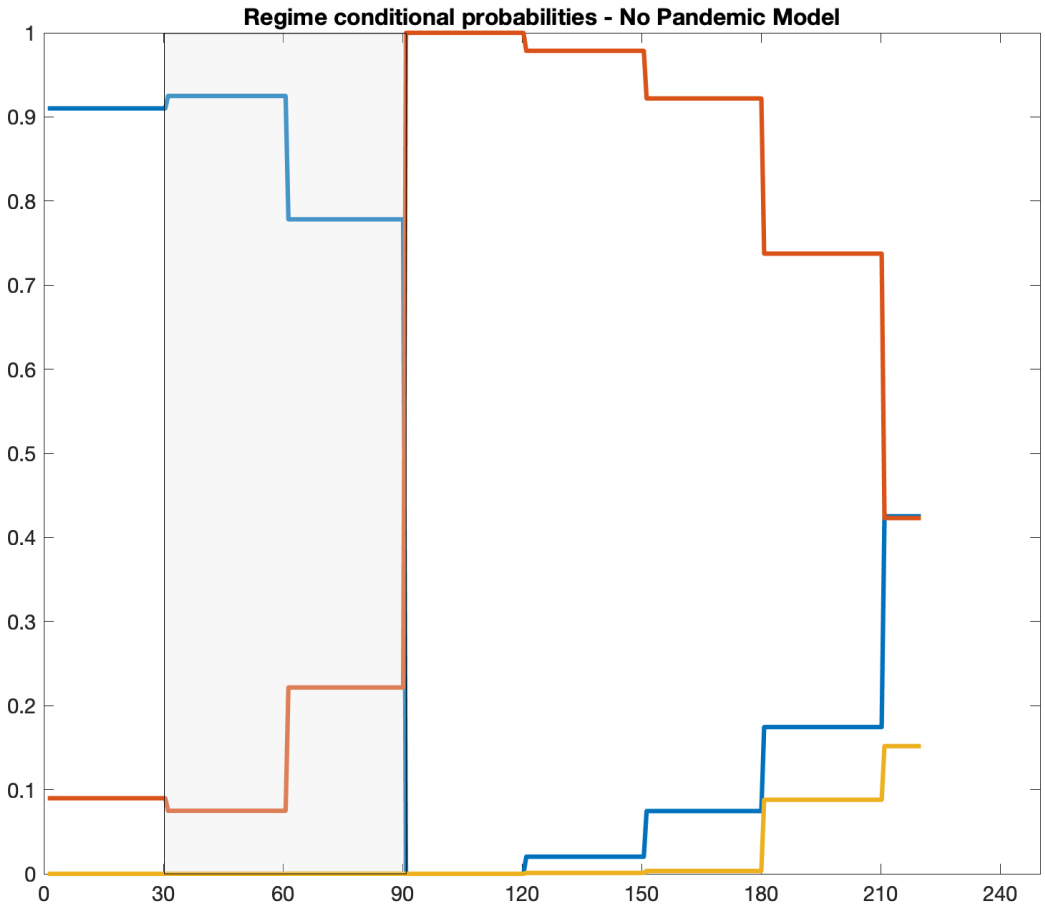


Figure 9: Conditional regime probabilities for the model without pandemic. Normal regime in blue, Recession regime in red, Boom regime in yellow. The shaded area corresponds to the NBER recession period. The sample period is January 1st through August 7th. The X-axis displays the day number.

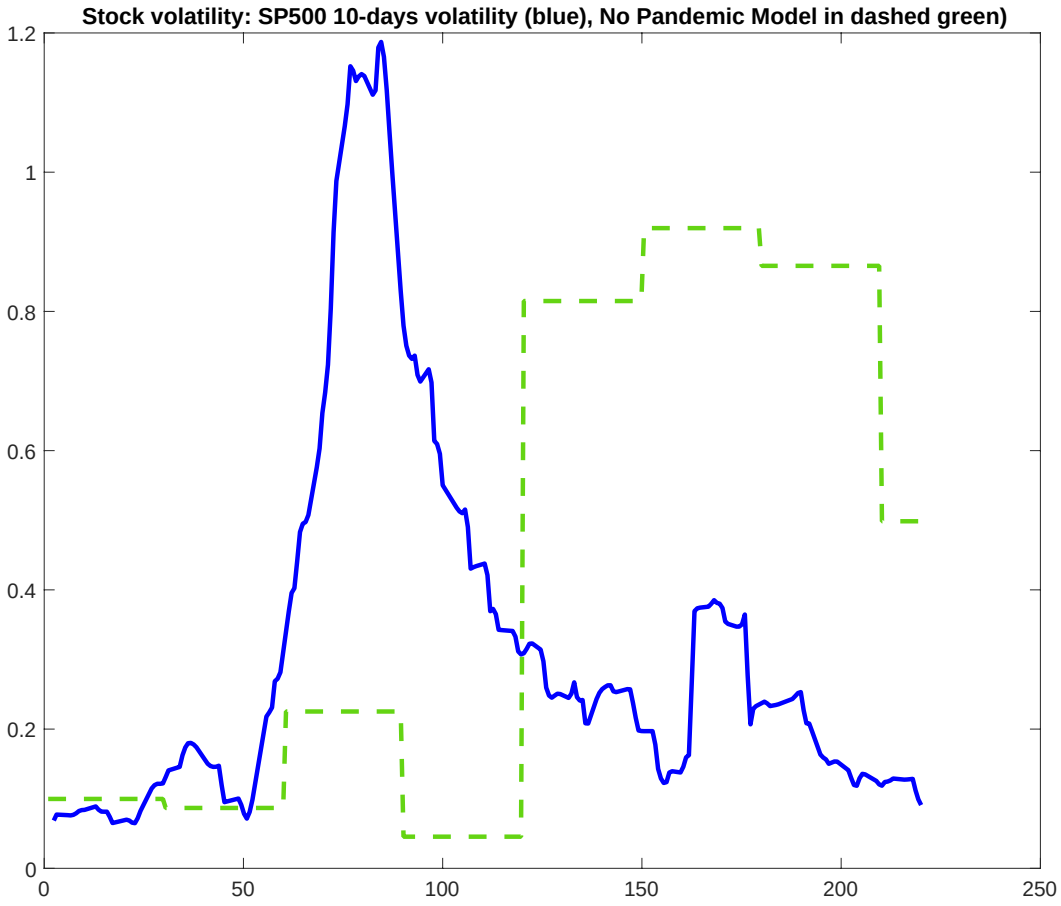


Figure 10: Volatility evolution in the model without pandemic. The sample period is January 1st through August 7th. The X-axis displays the day number.

Table 4: Estimated coeeficients for the SEIRD-LIFT model and the BDR-pandemic additional parameters. Sample period for estimation is January 2020 to July 2020.

BDR Model with Pandemic

| | estimated value | S.E. |
|---|---|---|
| $A_1^Y(1)$ | -0.0315006 | *tbc* |
| $A_2^Y(1)$ | -0.0008576 | *tbc* |
| $A_3^Y(1)$ | -0.6988067 | *tbc* |
| $A^C(1)$ | 0.0052649 | *tbc* |
| $A^G(1)$ | 0.0008880 | *tbc* |
| $a_i$ | 0.9625000 | *tbc* |
| $a_l$ | 0.9999878 | *tbc* |
| $\omega$ | 0.7552613 | *tbc* |
| $h$ | 0.9622143 | *tbc* |

SEIRD-SIP-LIFT model

| | estimated value | S.E. |
|---|---|---|
| $\beta_S$ | 2.3109725 | *tbc* |
| $\sigma$ | 0.0785581 | *tbc* |
| $\gamma$ | 0.0828043 | *tbc* |
| $\lambda$ | 0.0334010 | *tbc* |
| $\lambda_w$ | 0.5971951 | *tbc* |
| $\mu$ | 0.0000222 | *tbc* |
| $\nu^o$ | 0.0000047 | *tbc* |
| $\nu$ | 0.0000000 | *tbc* |
| $t_m$ | 66.4458234 | *tbc* |
| $\kappa_0$ (pre SIP) | 3.8165255 | *tbc* |
| $q$ | 0.0801839 | *tbc* |
| $q_2$ | 0.00084946 | *tbc* |
| $\kappa_1$ (during SIP) | 23.4286342 | *tbc* |
| $\kappa_2$ (post SIP) | 13.2838305 | *tbc* |
| $t_1$ | 61.5118993 | *tbc* |
| $t_2$ | 120.2493877 | *tbc* |
| $\tau_0$ | 18.8986733 | *tbc* |

## 4. Conclusion

In this paper we extended the BDRA model to accommodate unpredictable pandemic events such as the onset of an outbreak and the discovery of a vaccine, as well as associated mitigating policies such as SIP and LIFT. The BDRA-SEIRD-SIP-LIFT model was estimated using

economic and disease data from the COVID-19 outbreak. The estimated model was found to provide a close fit to variables targeted in the estimation, i.e., the number of new cases, the S&P 500 level and the index return volatility, as well as to non-targeted variables, i.e., the unemployment and consumption growth rates. At the same time, it generated a close match to 25 unconditional moments of economic time series, hence displayed consistency with long run statistical properties of economic and financial time series. Beliefs-dependent risk aversion was found to be critical for explanations of phenomena pre- and intra-COVID-19 outbreak.

While the model developed provides a comprehensive explanation for long term and short term features of the data, it leaves room for further improvements. Among the phenomena that are not explained are the level and behavior of the short rate and of the term structure of interest rates, both in the long run and during the COVID-19 outbreak. In that regard, the average interest rate and bond yields generated by the model are too high, and short term fluctuations too large to properly capture the data. A critical ingredient for that purpose is likely to be monetary policy. Actions by the Federal Reserve, e.g., pertaining to the federal funds rate, have undoubtedly shaped the response of fixed income markets during the outbreak. More generally, Quantitative Easing has had a profound effect on these markets since its inception in 2008. Incorporating such monetary policies in the analysis is an avenue for future research.

# 5. Appendix

## 5.1. Appendix A: the Stochastic SEIRD-SIP-LIFT Model

This appendix describes the SEIRD model under a SIP-LIFT policy, i,e,, a shelter-in-place (SIP) policy followed by a lifting (LIFT) of the restriction. This model extends Detemple (2022) by incorporating the unpredictable nature of pandemics and vaccine discoveries, captured by the Markov chain in Section 2.1. For generality we allow all the coefficients to be time-dependent.

In this model, populations in $\mathcal{S}, \mathcal{E}, \mathcal{I}$ transition to a sheltered stay-at-home state upon implementation of SIP and stay put until the policy is lifted. Sheltered (quarantined) populations

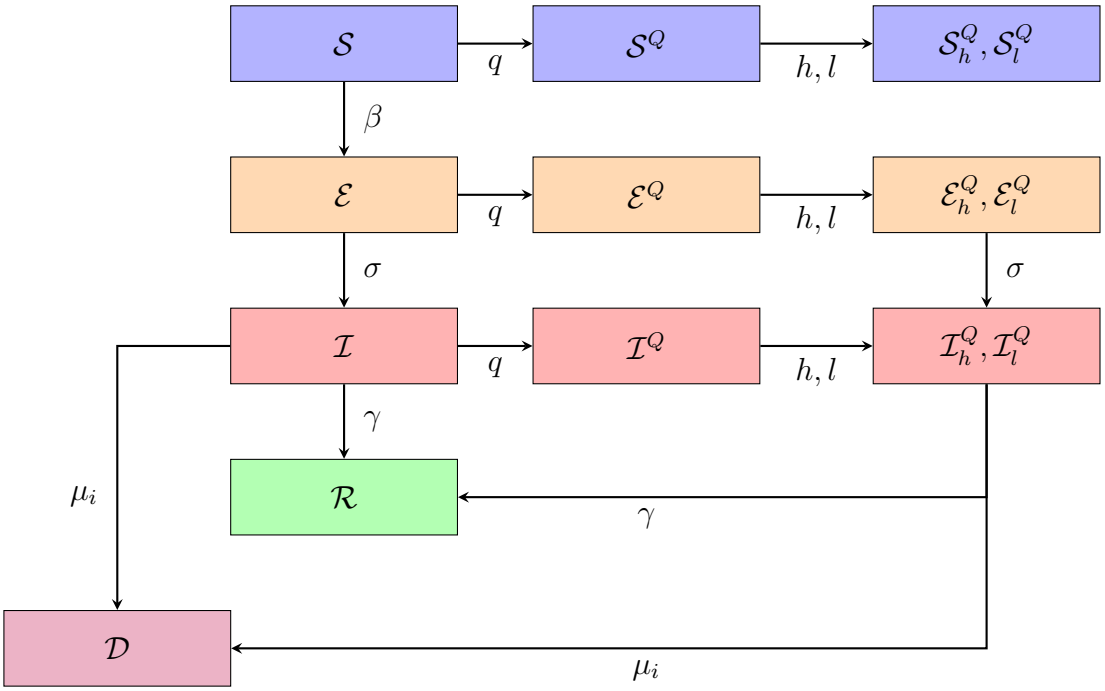


Figure 11: Flowchart for the SEIRD-SIP model.

are denoted with a superscript $Q$. Sheltered populations further split between work-at-home and laid-off populations, according to the fractions $h, l$ where $h + 1 = 1$. Work-at-home and laid-off populations are subscripted by $h$ and $l$, respectively. All infectious populations, sheltered and non-sheltered, split in three subgroups: asymptomatic, symptomatic mild, and symptomatic severe. Figure 5.1 illustrates the propagation mechanism across populations under SIP. Subgroups are not displayed.

We assume implementation of SIP takes time. The migration rate from $\mathcal{S}, \mathcal{E}, \mathcal{I}$ to the corresponding sheltered categories takes place at the constant rate $q$. Likewise when SIP is lifted, i.e., during LIFT, reverse migration from the sheltered categories to non-sheltered ones occurs at the constant rate $q_2$. In both cases, delays in implementation occur for a variety of reasons including the fact that policy recommendations are typically not uniformly adopted across states and, even when they are adopted, implementation may not be synchronous.

The evolution of populations under SIP-LIFT is described by the following system of ordinary differential equations

$$
\begin{aligned}
dp_s &= (\mu_t(1-p_d-p^Q_{s,h}-p^Q_{s,l}-p_s)-\beta_t p_i^{asy} p_s-(q_t+\nu_t^o+\nu_t 1_{\mathcal{V}_t})p_s)dt\\
dp^Q_{s,h} &= (q_t h p_s-(\nu_t^o+\nu_t 1_{\mathcal{V}_t})p^Q_{s,h})dt\\
dp^Q_{s,l} &= (q_t(1-h)p_s-(\nu_t^o+\nu_t 1_{\mathcal{V}_t})p^Q_{s,l})dt\\
dp_e &= (\beta_t p_i^{asy} p_s-(q_t+\mu_t+\sigma_t)p_e)dt\\
dp^Q_{e,h} &= (q_t h p_e-(\mu_t+\sigma_t)p^Q_{e,h})dt\\
dp^Q_{e,l} &= (q_t(1-h)p_e-(\mu_t+\sigma_t)p^Q_{e,l})dt\\
dp_i &= (\sigma_t p_e-(q_t+\mu_t+\mu_{it}+\gamma_t)p_i)dt\\
dp^Q_{i,h} &= (q_t h p_i+\sigma_t p^Q_{e,h}-(\mu_t+\mu_{it}+\gamma_t)p^Q_{i,h})dt\\
dp^Q_{i,l} &= (q_t(1-h)p_i+\sigma_t p^Q_{e,l}-(\mu_t+\mu_{it}+\gamma_t)p^Q_{i,l})dt\\
dp_r &= (\gamma_t(p_i+p^Q_{i,h}+p^Q_{i,l})-\mu_t p_r+(\nu_t^o+\nu_t 1_{\mathcal{V}_t})(p_s+p^Q_{s,h}+p^Q_{s,l}))dt\\
dp_d &= \mu_{it}(p_i+p^Q_{i,h}+p^Q_{i,l})dt
\end{aligned}
\tag{5.1}
$$

Several additional aspects of the propagation model under SIP are worth highlighting. First, all births are assigned to the susceptible classes. For sheltered susceptible $\mathcal{S}^Q$, as the birth rate equals the death rate, natural growth is null. For non-sheltered susceptible $\mathcal{S}$, natural growth is determined by the excess of birth in the surviving population $1-p_d$ net of birth assigned to the sheltered susceptible $p_s^Q$ over death in the non-sheltered susceptible $p_s$. Aggregating over sheltered and non-sheltered populations gives a flow of birth equal to $(1-p_d)\mu$. Second, populations in $\mathcal{S}^Q$ remain isolated, until the policy is lifted or they transition to $\mathcal{R}$ due to natural immunity or vaccination. Hence, they cannot be contaminated during that period. Third, $\mathcal{R}$ includes all recovered, naturally immune and vaccinated populations. Such individuals are immune to the disease, therefore apt to rejoin the workforce.[5] Fourth, $\mathcal{D}$ includes all the deceased from an infection: the fraction $p_d$ is the cumulative death toll as a fraction of the initial population $p_0 = 1$. Last, the transition from $\mathcal{S}$ to $\mathcal{E}$ does not depend on

[5]The formulation abstracts from issues of incomplete information pertaining to the health status of populations, in particular asymptomatic infectious ones.

sheltered individuals. Contamination, in fact, is entirely driven by non-sheltered asymptomatic individuals.

As previously indicated, lifting SIP, i.e., applying LIFT, reverses the migrations from $\mathcal{S}, \mathcal{E}, \mathcal{I}$ to $\mathcal{S}^Q, \mathcal{E}^Q, \mathcal{I}^Q$ in the model above. The reverse compliance rate $q_2$ replaces $q$. Applying that rate to sheltered symptomatic infectious populations does not affect the economic properties of the model, because such populations are not able to work by assumption.

## 5.2. Appendix B: Proofs

*Proof of Proposition 2.1.* The first order condition for population $j \in \{s, e, i, r\}$ is

$$\sum_{k=1}^{K} P_k \left(\frac{c_t}{a_j}\right)^{-R_k} = \frac{y\xi_t}{a_t} \equiv H_t. \tag{5.2}$$

where $y$ is a constant Lagrange multiplier, $\xi_t$ is the stochastic discount factor and $a_t = e^{-\beta_u t}$ is the subjective discount factor. Optimal consumption is $c_t = a_j I(H_t)$ where the function $I$, by concavity and Inada conditions, is the unique solution of the equation $\sum_{k=1}^{K} P_k I^{-R_k} = H$ and is independent of $j$.

Equilibrium in the consumption good market ensures $\sum_{j\in\{s,e,i,r\}} p_j a_j I(H_t) = C_t$. Solving gives $I(H_t) = C_t/p_c^a$ with $p_c^a = \sum_{j\in\{s,e,i,r\}} p_j a_j$. Hence, up to a constant, the stochastic discount factor is

$$\xi_t = \sum_{k=1}^{K} e^{-\beta_u t} \left(\frac{C_t}{p_{ct}^a}\right)^{-R_k} P_{kt}. \tag{5.3}$$

The jump in the SDF at $t = \tau_0$ is

$$\frac{\Delta\xi_t}{\xi_{t-}} = \sum_{k=1}^{K} \frac{e^{-\beta_u t} (C_t)^{-R_k} P_{kt}}{\sum_{k=1}^{K} e^{-\beta_u t} (C_t)^{-R_k} P_{kt}} \left((p_{ct}^a)^{R_k} - 1\right) dN_{12,t}^e \tag{5.4}$$

where $p_{ct}^a = 1 + \Delta_i(\lambda_i + \lambda_s a_i - 1)$ and $\Delta_i$ is the jump in $p_{it}$, and where we used $p_{ct-}^a = 1$. The coefficient $\lambda_s = (1-\lambda)(1-\lambda_w)$ is the fraction of symptomatic mild in the infectious

population, $\lambda_i = (1-\lambda)\lambda_w$ is the fraction of asymptomatic. The jump in the SPD at $t = \tau_1$ is null because $p_c^a$ is continuous at that point

Given the observed filtration, the SPD has dynamics,

$$d\xi_t/\xi_{t-} = -r_{t-}dt - \sum_{\alpha\in\{C,G,Y\}} \theta_{t-}^{\alpha} d\nu_t^{\alpha} - \theta_{t-}^{e_2} d\tilde{N}_{12,t}^{e}.$$

where $r$ is the interest rate, $\theta_t^{\alpha}$ for $\alpha \in \{C,G,Y\}$ is the market price of risk associated with the innovations $d\nu_t^{\alpha} = dW_t^{\alpha} - \sum_{k=1}^{3} \mu^{\alpha}(e_k) P_{kt} dt$ , $d\tilde{N}_{ij,t}^{e} = dN_{ij,t}^{e} - \Lambda_{ij}^{e} dt$ are the jump innovations and $\theta_t^{e_j}$ are the market prices of jump risks. Taking derivatives on both sides of (5.3) and identifying drift, jump, and volatility coefficients for diffusion and jump risks yields the formulas announced. In particular,

$$\theta_{t-}^{e_2} = \sum_{k=1}^{K} \frac{e^{-\beta_u t} (C_t)^{-R_k} P_{kt}}{\sum_{k=1}^{K} e^{-\beta_u t} (C_t)^{-R_k} P_{kt}} \left(1 - (p_{ct}^a)^{R_k}\right) \tag{5.5}$$

and $\theta_{t-}^{e_3} = 0$ . The interest rate has the jump premium component $\theta_{t-}^{e_2}\Lambda_{12}$ . □

**Proposition 5.1.** *For $\alpha \in \{C,G,Y\}$ , define the diagonal matrix $diag(\mu^{\alpha})$ with diagonal $\mu^{\alpha}$ , and the identity matrix $I_K$ of dimension $K$ . Also introduce the $K \times K$ matrix function $\Upsilon(t, s_t^e)$ with elements,*

$$\Upsilon_{ij}(t, s_{t-}^e) = e_i' (e_i' \otimes I_K) G(t, s_{t-}^e) (e_i \otimes I_K) e_j \tag{5.6}$$

*where*

$$G(t, e_1) \equiv G_1^o + \Lambda_{12}^e G_1^e(t) \tag{5.7}$$

*with $G_1^o \equiv (\Phi^o)^{-1}$ ,*

$$G_1^e(t) \equiv -(\Phi^o)^{-1} (\Phi^o + I_{K^2}\Lambda_{12}^e)^{-1} + \int_t^{\infty} e^{-\Phi^o(v-t)} G(v, e_2) e^{-\Lambda_{12}^e(v-t)} dv \tag{5.8}$$

(5.9)

$$G(t,e_2) \equiv \int_t^\infty e^{-\Phi^o(v-t)-\int_t^v \Phi^e(u,e_2)du}\left(e^{-\Lambda^e_{23}(v-t)}I_{K^2}+\Lambda^e_{23}\int_t^v e^{-\Phi^o(s-t)-\int_t^s \Phi^e(u,e_2)du-\Lambda^e_{23}(s-t)}ds\right)dv$$

(5.10) $$G(t,e_3) \equiv \int_t^\infty e^{-\Phi^o(s-t)-\int_t^s \Phi^e(u,e_3)du}ds$$

(5.11) $$-\Phi^o = (diag_K[-g_k]\otimes I_K)+(I_K\otimes\Lambda')+(diag_K[\kappa-R_k]\otimes diag(\mu^C_k))+(I_K\otimes diag(\mu^G_k))$$

(5.12) $$-\Phi^e(t,e_j) = diag_K[\eta^e_k(t,e_j)]\otimes I_K$$

(5.13) $$\eta^e_k(t,e_j) = \left(\left((\kappa-R_k)\,A^C_k+A^G_k\right)\frac{\mu^{p^e_w}(t,e_j)}{p^e_{wt}}+R_k\frac{\mu^{p^a_{ct}}(t,e_j)}{p^a_{ct}}\right)1_{\{j\neq 1\}}.$$

*The functions* $(\mu^{p^e_w}(t,e_j),\mu^{p^a_{ct}}(t,e_j))$ *are the drifts of* $(p^e_w,p^a_c)$ *, and*

(5.14) $$g_k = \beta_u - \frac{1}{2}(\kappa-R_k)(\kappa-1-R_k)(\sigma^C)^2$$

(5.15) $$\mu^G_{ok} = \mu^D_{ok} - \kappa\mu^C_{ok} + \frac{1}{2}\rho\sigma^D\sigma^C(1-\kappa)$$

(5.16) $$\mu^\alpha_{o,k} = \mu^\alpha_o(e_k), \qquad \mu^\alpha_{k,t} = \mu^\alpha_{o,k} + \eta^e_k(t,s^e_t))$$

*If* $\Upsilon_{ij}(t,s^e_{t-})$ *is finite, the stock price is* $S_t = D_t Z_t'\Upsilon(t,s^e_{t-})P_t$ *where* $Z_t = q_{kt}/P_{kt}$ *.*

*Proof of Proposition 5.1.* Using $G_tC^\kappa_t = D_t$ enables us to write the stock price as

$$\frac{S_t}{D_t} = \frac{E_{t-}\left[\int_t^\infty\left(\sum_{k=1}^K e^{-\beta_u v}\left(C_v/p^a_{cv}\right)^{-R_k}P_{kv}\right)D_v dv\right]}{\sum_{k=1}^K H_{k,t}} = \frac{\int_t^\infty V^H(t,v)\,dv}{\sum_{k=1}^K H_{k,t}},$$

with $V^H(t,v)\equiv\sum_{k=1}^K V^H_k(t,v)$ , $V^H_k(t,v)\equiv E_{t-}[H_{k,v}]$ , $H_{k,v}\equiv e^{-\beta_u v}\left(p^a_{cv}\right)^{R_k}C^{\kappa-R_k}_v P_{kv}G_v$ .

Let $\tau_0\equiv\inf\{v\geqslant 0:\Delta N_{12v}=1\}$ be the time a pandemic is triggered. Then define $L_t\equiv(L_{1t},\ldots,L_{Kt})$ with $L_{kt}\equiv e^{-\beta t}\left(p^a_{ct}\right)^{R_k}C^{\kappa-R_k}_t G_t$ , and $N_t\equiv L_t\otimes P_t$ with $P_t\equiv(P_{1t},\ldots,P_{Kt})'$ . The operator $\otimes$ is the Kronecker product. The Kronecker product of matrices (or vectors) $A$ and $B$ is the matrix $A\otimes B = [A_{ij}B]_{i,j=1,\ldots,K}$ . The vector $N$ multiplies the vector of posterior probabilities $P_t$ by $e^{-\beta_u t}\left(p^a_{ct}\right)^{R_k}C^{\kappa-R_k}_t G_t, k=1,...,K$ and stacks the resulting vectors on top of each other. Also, if $e_k\equiv(0,\ldots,1,\ldots,0)'$ denotes the $k^{th}$ unit vector, let

$\mathbf{e} \equiv \ vec\left([e_1, \ldots, e_K]\right) \equiv \ \left(e_1', \ldots, e_K'\right)'$ be the $K^2$-dimensional vector stacking unit vectors on top of each other.[6] Finally, define the vector of expected growth rates $\left(\bar{\mu}^\alpha\right)' \equiv \ [\mu_1^\alpha, \ldots, \mu_k^\alpha]$, the diagonal matrix $\text{diag}\left(\bar{\mu}^\alpha\right)$ with diagonal $\bar{\mu}^\alpha$, the $k^{th}$ eigenvalue $\delta_k(A)$ of an arbitrary matrix $A$, and the identity matrix $I_K$ of dimension $K$. Define $\widehat{\eta}_{kt} \equiv \ \widehat{\eta}^o_{kt} + \widehat{\eta}^e_{kt}$ where

$$\widehat{\eta}^o_{kt} \equiv (\kappa - R_k)\left(\widehat{\mu}^C_{o,t} + \frac{1}{2}(\kappa - 1 - R_k)\left(\sigma^C\right)^2\right) - \beta_u + \widehat{\mu}^G_{o,t}$$
$$\widehat{\eta}^e_{kt} = \widehat{\eta}^e_k(t, s^e_{t-}) = \left(\left((\kappa - R_k)\,\widehat{A}^C_t + \widehat{A}^G_t\right)\frac{\mu^{p^e_w}(t, s^e_{t-})}{p^e_{wt}} + R_k \frac{\mu^{p^a_{ct}}(t, s^e_{t-})}{p^a_{ct}}\right) 1_{\mathcal{E}_t},$$

where for $\alpha \in \{C, G\}$, $\widehat{\mu}^\alpha_{o,t} = \sum_{k=1}^K \mu^\alpha_{o,k} P_{kt}$ and $\widehat{A}^\alpha_t = \sum_{k=1}^K A^\alpha_k P_{kt}$. With these definitions and the notation above, the dynamics of $L$ and $P$ are

$$\begin{aligned} dL_t &= \text{diag}_K\left[\widehat{\eta}_{kt}\right] L_t dt + \left(\left(\text{diag}_K\left[\kappa - R_k\right]\right)\sigma^C d\nu^C_t + I_K \sigma^G d\nu^G_t\right) L_t \\ &\equiv \mu^L_t L_t dt + \sigma^{L_C}_t L_t d\nu^C_t + \sigma^{L_G}_t L_t d\nu^G_t, \\ dP_t &= \Lambda' P_t dt + \sum_{\alpha \in \mathcal{I}} \sigma^{P\alpha}_t P_t d\nu^\alpha_t, \end{aligned}$$

where $\sigma^{P\alpha}_t \equiv \text{diag}_K\left[\Delta^\alpha_{kt}\right]$ where $\Delta^\alpha_{kt} = (\mu^\alpha_{k,t} - \sum_{k=1}^K \mu^\alpha_{kt} P_{kt})/\sigma^\alpha$ and $\text{diag}_K[a_k] \equiv \text{diag}(a)$ for $a' \equiv [a_1, \ldots, a_K]$. Applying Ito's lemma to the Kronecker product $N_t \equiv L_t \otimes P_t$ gives, with $\mathcal{I} \equiv \{C, G, Y\}$ and $\mathcal{J} \equiv \{C, G\}$,

$$\begin{aligned} dN_t &= (dL_t \otimes P_t) + (L_t \otimes dP_t) + (dL_t \otimes dP_t) = \left(\left(\mu^L_t \otimes I_K\right) dt + \sum_{\alpha \in \mathcal{J}} \left(\sigma^{L\alpha}_t \otimes I_K\right) d\nu^\alpha_t\right) N_t \\ &+ \left((I_K \otimes \Lambda')\, dt + \sum_{\alpha \in \mathcal{I}} \left(I_K \otimes \sigma^{P\alpha}_t\right) d\nu^\alpha_t\right) N_t + \sum_{\alpha \in \mathcal{J}} \left(\sigma^{L\alpha}_t \otimes \sigma^{P\alpha}_t\right) N_t dt \\ &\equiv -\Phi N_t dt + \sum_{\alpha \in \mathcal{I}} \sigma^{N\alpha}_t N_t d\nu^\alpha_t, \end{aligned} \tag{5.17}$$

[6] The vec-operator stacks the columns of a matrix $A$ on top of each other, $vec([A_1, \ldots, A_K]) = (A_1', \ldots, A_K')'$. When $A = I_K$, the $K$-dimensional identity matrix, $vec(I_K) = vec([e_1, \ldots, e_K]) = \mathbf{e}$.

where $-\Phi \equiv \left(\mu_t^L \otimes I_K\right) + \left(I_K \otimes \Lambda'\right) + \sum_{\alpha \in \mathcal{J}} \left(\sigma_t^{L\alpha} \otimes \sigma_t^{P\alpha}\right)$. Using

$$\widehat{\eta}_{kt}^o \equiv (\kappa - R_k)\left(\widehat{\mu}_{o,t}^C + \frac{1}{2}(\kappa - 1 - R_k)\left(\sigma^C\right)^2\right) - \beta + \widehat{\mu}_{o,t}^G \equiv (\kappa - R_k)\,\widehat{\mu}_{o,t}^C - g_k + \widehat{\mu}_{o,t}^G$$

gives $-\Phi(t, s_t^e) = -\Phi^o - \Phi^e(t, s_t^e)$ where with $g_k \equiv -\frac{1}{2}(\kappa - R_k)(\kappa - 1 - R_k)\left(\sigma^C\right)^2 + \beta$ and

$$\begin{aligned}
\eta_k^o &\equiv (\kappa - R_k)\,\mu_{o,k}^C - g_k + \mu_{o,k}^G \\
\eta_k^e(t, s_t^e) &\equiv \left(\left((\kappa - R_k)\,A_k^C + A_k^G\right)\frac{\mu^{p_w^e}(t, e_j)}{p_{wt}^e} + R_k \frac{\mu^{p_{ct}^a}(t, e_j)}{p_{ct}^a}\right) 1_{\{s_t^e \neq e_1\}}
\end{aligned}$$

$$\begin{aligned}
-\Phi^o &= \left(\mathrm{diag}_K\left[\eta_{kt}^o\right] \otimes I_K\right) + \left(I_K \otimes \Lambda'\right) + \left(\mathrm{diag}_K\left[\kappa - R_k\right] \otimes \left(\mathrm{diag}\left(\bar{\mu}^C\right) - \widehat{\mu}_{o,t}^C I_K\right)\right) \\
&\quad + \left(I_K \otimes \left(\mathrm{diag}\left(\bar{\mu}^G\right) - \widehat{\mu}_{o,t}^G I_K\right)\right) \\
&= \left(\mathrm{diag}_K\left[-g_k\right] \otimes I_K\right) + \left(I_K \otimes \Lambda'\right) + \left(\mathrm{diag}_K\left[\kappa - R_k\right] \otimes \mathrm{diag}\left(\bar{\mu}^C\right)\right) \\
&\quad + \left(I_K \otimes \mathrm{diag}\left(\bar{\mu}^G\right)\right), \\
-\Phi^e\left(t, s_t^e\right) &= \left(\mathrm{diag}_K\left[\eta_{kt}^e\right] \otimes I_K\right),
\end{aligned}$$

$$\begin{aligned}
\sigma_t^{N_C} &\equiv \left(\sigma_t^{LC} \otimes I_K\right) + \left(I_K \otimes \sigma_t^{pC}\right) = \left(\mathrm{diag}_K\left[\kappa - R_k\right] \otimes I_K\right)\sigma^C + \left(I_K \otimes \sigma_t^{PC}\right), \\
\sigma_t^{NG} &\equiv \left(\sigma_t^{L_G} \otimes I_K\right) + \left(I_K \otimes \sigma_t^{pG}\right) = \left(I_K \otimes I_K\right)\sigma^G + \left(I_K \otimes \sigma_t^{PG}\right), \\
\sigma_t^{NY} &\equiv I_K \otimes \sigma_t^{pY} = I_K \otimes \sigma_t^{PY}.
\end{aligned}$$

The final expression for $\Phi^o$ and $\Phi^e$ above is obtained by cancelling the terms involving $\widehat{\mu}_{o,t}^C, \widehat{A}_t^C, \widehat{A}_t^G$. This follows because the Kronecker product is bilinear and associative, $(A \otimes (B + C)) = (A \otimes B) + (A \otimes C)$, and $(\alpha A \otimes B) = (A \otimes \alpha B) = \alpha\,(A \otimes B)$ for scalar $\alpha$ and matrices $A, B$. Next define $\mathcal{G}_t = \mathcal{F}_t \otimes \mathcal{F}_\infty^{s^e}$ where $\mathcal{F}_t^{s^e}$ is the natural filtration of $s_t^e$.

From Equation (5.17) the conditional mean $V^N(t, s) \equiv E\left[N_v \middle| \mathcal{G}_t\right]$ solves $dV_j^N(t, v) = -\left(\Phi^o + \Phi^e(v, e_j)\right) V^N(t, v)\,dv$ with initial condition $V^N(t, t) = N_t$. The solution is $V^N(t, v) =$

$\exp\left(-\Phi^o(v-t) - \int_t^v \Phi^e\left(u, s^e_{u-}\right) du\right) N_t$ . Thus,

$$V^H(t,s) = \sum_{k=1}^{K} V_k^H(t,s) = \mathbf{e}'\left(e^{-\Phi^o(s-t)}\right) E\left[e^{-\int_t^s \Phi^e\left(u,s^e_{u-}\right)du}\middle| \mathcal{F}^{s^e}_{t-}\right] N_t,$$

where the matrix exponential $e^{-\Phi^o(s-t)} E\left[e^{-\int_t^s \Phi^e_j\left(u,s^e_{u-}\right)du}\middle| \mathcal{F}^{s^e}_{t-}\right]$ is a $K^2 \times K^2$ diagonal matrix because $\Phi$ is $K^2 \times K^2$ diagonal, and the vector $\mathbf{e}' \equiv vec\left([e_1, \ldots, e_K]\right)$ selects element $k$ in block $k$ to construct the sum $\sum_{k=1}^K V_k^H(t,s)$ .

Let $\tau_0 = \inf\{v > 0 : \Delta N^e_{12} = 1\}$ and $\tau_1 = \inf\{v > \tau_0 : \Delta N^e_{23} = 1\}$ . Integration then gives with $\vartheta_j(s,t) \equiv e^{-\Phi^o(s-t)} e^{-\int_t^s \Phi^e(u,e_j)du}$ ,

$$\frac{S_t}{D_t} = \begin{cases} \frac{E\left[\mathbf{e}'\left(\int_t^\infty \vartheta_3(s,t)ds\right)\middle|\mathcal{F}^{s^e}_{t-}\right]N_{3t}}{\mathbf{e}'N_{3t}} & \text{if } t \geqslant \tau_1 \\ \frac{E\left[\mathbf{e}'\left(\int_t^{\tau_1} \vartheta_2(s,t)ds + \int_{\tau_1}^\infty \vartheta_3(s,t)ds\right)\middle|\mathcal{F}^{s^e}_{t-}\right]N_{2t}}{\mathbf{e}'N_{2t}} & \text{if } \tau_0 \leqslant t < \tau_1 \\ \frac{E\left[\mathbf{e}'\left(\int_t^{\tau_0} \vartheta_1(s,t)ds + \int_{\tau_0}^{\tau_1} \vartheta_2(s,t)ds + \int_{\tau_1}^\infty \vartheta_3(s,t)ds\right)\middle|\mathcal{F}^{s^e}_{t-}\right]N_{1t}}{\mathbf{e}'N_{1t}} & \text{if } t < \tau_0 \end{cases}$$

provided the integrals exists.

To proceed, define $G(t, s^e_{t-}) \equiv \int_t^\infty e^{-\Phi^o(s-t)} E\left[e^{-\int_t^s \Phi^e\left(u,s^e_{u-}\right)du}\middle| \mathcal{F}^{s^e}_{t-}\right] ds$ . If $t > \tau_1$ , then $s^e_t = s^e_{t-} = e_3$ because $\Lambda^e_{31} = \Lambda^e_{32} = 0$ and,

$$G(t, e_3) = \int_t^\infty e^{-\Phi^o(s-t)} e^{-\int_t^s \Phi^e(u,e_3)du} ds.$$

If $\tau_1 \geqslant t > \tau_0$ , then $s^e_{t-} = e_2$ , and because $P\left(\tau_1 \in dv \middle| s^e_{t-} = e_2\right) = \Lambda^e_{23} e^{-\Lambda^e_{23}(v-t)}$ ,

$$\begin{aligned} G(t,e_2) =& E\left[\int_t^{\tau_1} e^{-\Phi^o(s-t)} e^{-\int_t^s \Phi^e\left(u,s^e_{u-}\right)du}\middle| \mathcal{F}^e_{t-}\right] + E\left[e^{-\Phi^o(\tau_1-t)} e^{-\int_t^{\tau_1} \Phi^e(u,e_2)du} G(\tau_1,e_3)\middle| \mathcal{F}^e_{t-}\right] \\ =& \Lambda^e_{23} \int_t^\infty \left(\int_t^v e^{-\Phi^o(s-t)-\int_t^s \Phi^e(u,e_2)du} ds\right) e^{-\Lambda^e_{23}(v-t)} dv \\ &+ \Lambda^e_{23} \int_t^\infty e^{-\Phi^o(v-t)-\int_t^v \Phi^e(u,e_2)du} G(v,e_3) e^{-\Lambda^e_{23}(v-t)} dv \\ =& \int_t^\infty e^{-\Phi^o(v-t)-\int_t^v \Phi^e(u,e_2)du} \left(e^{-\Lambda^e_{23}(v-t)} I_{K^2} + \Lambda^e_{23} \int_t^v e^{-\Phi^o(s-t)-\int_t^s \Phi^e(u,e_2)du - \Lambda^e_{23}(s-t)} ds\right) dv \end{aligned}$$

If $t < \tau_0$, $s^e_{t-} = e_1$, and hence, $\Phi^e(t, e_1) = 0$. Then as $P\left(\tau_0 \in dv \middle| s^e_{t-} = e_1\right) = \Lambda^e_{12} e^{-\Lambda_{12}(t-v)}$,

$$\begin{aligned}
G(t,e_1) =& E\left[\int_t^{\tau_0} e^{-\Phi^o(s-t)-\int_t^s \Phi^e(u,e_1)du} ds \middle| \mathcal{F}^{s^e}_{t-}\right] + E\left[\int_{\tau_0}^{\infty} e^{-\Phi^o(s-t)-\int_t^s \Phi^e(u,s^e_{u-})du} ds \middle| \mathcal{F}^{s^e}_{t-}\right] \\
=& \Lambda^e_{12}\int_t^{\infty}\int_t^{v} e^{-\Phi^o(s-t)} ds e^{-\Lambda^e_{12}(v-t)} dv + \Lambda^e_{12}\int_t^{\infty} e^{-\Phi^o(v-t)} G(v,e_2) e^{-\Lambda^e_{12}(v-t)} dv \\
=& -\Lambda^e_{12}\left(\Phi^o\right)^{-1}\int_t^{\infty}\left(e^{-\Phi^o(v-t)} - I_{K^2}\right) e^{-\Lambda^e_{12}(v-t)} dv + \Lambda^e_{12}\int_t^{\infty} e^{-\Phi^o(v-t)} G(v,e_2) e^{-\Lambda^e_{12}(v-t)} dv \\
=& \left(\Phi^o\right)^{-1}\left(I_{K^2} - \Lambda^e_{12}\left(\Phi^o + I_{K^2}\Lambda^e_{12}\right)^{-1}\right) + \Lambda^e_{12}\int_t^{\infty} e^{-\Phi^o(v-t)} G(v,e_2) e^{-\Lambda^e_{12}(v-t)} dv \\
=& \left(\Phi^o\right)^{-1} + \Lambda^e_{12}\left(-\left(\Phi^o\right)^{-1}\left(\Phi^o + I_{K^2}\Lambda^e_{12}\right)^{-1} + \int_t^{\infty} e^{-\Phi^o(v-t)} G(v,e_2) e^{-\Lambda^e_{12}(v-t)} dv\right) \\
=& G^o_1 + \Lambda^e_{12} G^e_1(t)
\end{aligned}$$

Next, note that $N_t = (L_t \otimes P_t) = vec\left(P_t L_t'\right) = \left(L_t' \otimes I_K\right) P_t$. Therefore,

$$\mathbf{e}' N_t = L_t' P_t = E_t\left[\left(\sum_k e^{-\beta t}\left(p^a_{ct}\right)^{R_k} C_t^{-R_k} P_{kt}\right) D_t\right]$$

and $N_t/\mathbf{e}'N_t = \left(Z_t \otimes I_K\right) P_t$ where $Z_t = [Z_{1t}, \ldots, Z_{Kt}]$ with $Z_{kt} = q_{kt}/P_{kt}$, $k = 1, ..., K$. Let $\Upsilon_{ij}\left(t, s^e_t\right) \equiv e_i'\left(e_i' \otimes I_K\right) G(t, s^e_t)\left(e_i \otimes I_K\right) e_j$ be element ij of the $K \times K$ matrix function $\Upsilon\left(t, s^e_t\right)$. With this notation, $\mathbf{e}'\Phi^{-1} N_t/\mathbf{e}'N_t = Z_t'\Upsilon\left(t, s^e_t\right) P_t$ and,

$$\frac{S_t}{D_t} = \begin{cases} Z_t'\Upsilon\left(t, s^e_t\right) P_t & \text{if } \Upsilon_{ij}\left(t, s^e_t\right) \text{ is finite} \\ \infty & \text{otherwise} \end{cases}.$$

Applying Ito's lemma gives the volatility,

$$\sigma_t' = \left(\kappa\sigma^C, \sigma^G, 0\right) + \frac{Z_t'\Upsilon\mathcal{D}_t P_t}{Z_t'\Upsilon P_t} + \frac{p_t'\Upsilon'\mathcal{D}_t Z_t}{Z_t'\Upsilon P_t},$$

$$\mathcal{D}_t Z_t = \frac{\mathcal{D}_t L_t}{P_t' L_t} - L_t \frac{P_t' \mathcal{D}_t L_t + L_t' \mathcal{D}_t P_t}{\left(P_t' L_t\right)^2} = \left(\frac{1}{P_t' L_t} - L_t \frac{P_t'}{\left(P_t' L_t\right)^2}\right) \mathcal{D}_t L_t - L_t \frac{L_t' \mathcal{D}_t P_t}{\left(P_t' L_t\right)^2}.$$

Using $\mathcal{D}_t^Y L_t = 0$ and $\mathcal{D}_t^\alpha P_t = \sigma_t^{P,\alpha} P_t$ gives $\sigma_t' = \left(\rho\sigma^D + \sigma_t^{SCR} + \sigma_t^{SCG}, \sqrt{1-\rho^2}\sigma^D + \sigma_t^{SGG}, \sigma_t^{SYG}\right)$ with,

$$\sigma_t^{SCR} \equiv \frac{P_t' \Upsilon'}{Z_t' \Upsilon P_t} \left(\frac{1}{P_t' L_t} - L_t \frac{P_t'}{\left(P_t' L_t\right)^2}\right) \mathcal{D}_t^C L_t = \left(\frac{Z_t' \mathrm{diag}_K\left[-R_k\right] \Upsilon P_t}{Z_t' \Upsilon P_t} - Z_t' \mathrm{diag}_K\left[-R_k\right] P_t\right) \sigma^C,$$

$$\sigma_t^{S\alpha G} \equiv \left(\frac{Z_t' \Upsilon}{Z_t' \Upsilon P_t} - \frac{P_t' \Upsilon'}{Z_t' \Upsilon P_t} L_t \frac{\left(L_t\right)'}{\left(P_t' L_t\right)^2}\right) \mathcal{D}_t^\alpha P_t = \left(\frac{Z_t' \Upsilon}{Z_t' \Upsilon P_t} - Z_t'\right) \sigma_t^{P,\alpha} P_t.$$

The right hand sides of these equalities are obtained by using $\mathcal{D}_t^C L_t = \mathrm{diag}_K\left[-R_k\right] L_t \sigma^C$, $\mathcal{D}_t^\alpha P_t = \sigma_t^{P,\alpha} P_t$ and $Z_t = L_t / P_t' L_t$. Simplifying gives the formulas announced. □

**Remark 5.2.** *Note that*

$$M_t^e = e^{-\Phi^o t - \int_0^t \Phi^e(u, s_{u-}^e) du} G(t, s_{t-}^e) + \int_0^t e^{-\Phi^o v - \int_0^v \Phi^e(u, s_{u-}^e) du} dv$$

*is a $\mathcal{F}_\cdot^{s^e}$-martingale. Using Ito's lemma and $E[dM_t^e | \mathcal{F}_t^{s^e}] = 0$ gives*

$$\left(\Phi^o + \Phi^e(t, s_{t-}^e)\right) G(t, s_{t-}^e) = \frac{\partial}{\partial t} G(t, s_{t-}^e) + I_{K^2} + \sum_{j=1}^{3} \left(G(t, e_j) - G(t, s_{t-}^e)\right) \left(s_{t-}^e\right)' \Lambda^e e_j,$$

*with boundary condition $G(\infty, \cdot) = \mathbf{0}_{K^2}$, where $\mathbf{0}_{K^2}$ is a square matrix of zeros of dimension $K^2$. Evaluating this at all possible values of $s_t^e \in \{e_1, e_2, e_3\}$ gives the ODE*

$$d\overline{G}(t) = \left(\widetilde{\Phi}(t) \overline{G}(t) - I_{K^2}\right) dt; \quad \overline{G}(\infty) = \mathbf{1}_3 \otimes \mathbf{0}_{K^2}$$

*where $\overline{G}(t)' \equiv [G(t, e_1)', G(t, e_2)', G(t, e_3)']$ and $\widetilde{\Phi}(t) \equiv \mathrm{diag}_3\left[\Phi(t, e_j)\right] + \left(\Lambda^e \otimes I_{K^2}\right)$. Integrating (if the RHS exists) and using the boundary condition gives*

$$\overline{G}(t) = \int_t^\infty e^{-\int_t^v \widetilde{\Phi}(u) du} dv \left(\mathbf{1}_3 \otimes I_{K^2}\right) \tag{5.18}$$

$$(5.19) \qquad G(t, s^e_{t-}) = \left( \left( s^e_{t-} \right)' \otimes I_{K^2} \right) \int_t^\infty e^{-\int_t^v \tilde{\Phi}(u)du} dv \left( \mathbf{1}_3 \otimes I_{K^2} \right),$$

*and therefore,*

$$(5.20) \qquad \Upsilon_{ij}(t, s^e_{t-}) = e_i' \left( e_i' \otimes I_K \right) \left( \left( s^e_{t-} \right)' \otimes I_{K^2} \right) \int_t^\infty e^{-\int_t^v \tilde{\Phi}(u)du} dv \left( \mathbf{1}_3 \otimes I_{K^2} \right) \left( e_i \otimes I_K \right) e_j$$

*This shows how to calculate the function* $G(t, s^e_{t-})$ *in a general setting without further restrictions on the matrix* $\Lambda^e$ *.*

## 5.3. Appendix C: Orthogonalization

The state variables $X_t' \equiv [C_t, G_t, Y_t]$ are orthogonalized state variables derived from macro variables $\widetilde{X}_t \equiv [C_T, D_t, E_t]$, where $C_t$ is per capita consumption, $D_t$ aggregate dividends, and $E_t$ unemployment. Macro state variables have covariance matrix $\Sigma$ and dynamics

$$(5.21) \qquad d\widetilde{X}_t = \text{diag}[\widetilde{X}_t] \left( \left( \overline{\mu}^{\tilde{X}} s^m_t + \widetilde{A}(s^m_t) \frac{\mu^{p^e_w}(t, s^e_t)}{p^e_{wt}} 1_{\mathcal{E}_t} \right) dt + \Sigma dW_v \right)$$

where $\widetilde{A}'(s^m_t) = [A^C(s^m_t), A^D(s^m_t), A^E(s^m_t)]$, $\overline{\mu}^{\tilde{X}}$ is a $3 \times 3$ matrix with rows composed of expected growth rates in each regime, $\Sigma$ is the Choleski decomposition of the covariance matrix $\Sigma\Sigma'$,

$$(5.22) \qquad \overline{\mu}^{\tilde{X}} = \begin{bmatrix} \mu_1^C & \mu_2^C & \mu_3^C \\ \mu_1^D & \mu_2^D & \mu_3^D \\ \mu_1^E & \mu_2^E & \mu_3^E \end{bmatrix}, \; \Sigma \equiv \begin{bmatrix} \sigma^C & 0 & 0 \\ \rho^{CD}\sigma^D & \sqrt{1 - (\rho^{CD})^2}\sigma^D & 0 \\ \rho^{CE}\sigma^E & \rho^{DE}\sigma^E & \sqrt{1 - (\rho^{CE})^2 - (\rho^{DE})^2}\sigma^E \end{bmatrix},$$

and $W_t' = \left[W^C, W^G, W^Y\right]$ is a 3-dimensional vector of independent Brownian motions. To find the orthogonalized state variables, define $\widetilde{x}_{it} = \log \widetilde{X}_{it}$ and note that

$$d\widetilde{x}_t = \left(\overline{\mu}^{\widetilde{X}} s_t^m - \frac{1}{2}\mathrm{dg}\left[\Sigma\Sigma'\right] + A(s_t^m)\frac{\mu^{p_w^e}(t, s_t^e)}{p_{wt}^e} 1_{\mathcal{E}_t}\right) dt + \Sigma dW_t$$

where for a $m \times m$ square matrix $B$, $\mathrm{dg}[B]$ is the $m \times 1$ vector of diagonal elements of $B$. Then define $\widehat{x}_t = K\widetilde{x}_t$ with $K = \mathrm{diag}[\mathrm{dg}[\Sigma]]\Sigma^{-1}$ and note that

$$d\widehat{x}_t = K\left(\overline{\mu}^{\widetilde{X}} s_t^m - \frac{1}{2}\mathrm{dg}\left[\Sigma\Sigma'\right] + \widetilde{A}(s_t^m)\frac{\mu^{p_w^e}(t, s_t^e)}{p_{wt}^e} 1_{\mathcal{E}_t}\right) dt + \mathrm{diag}[\mathrm{dg}[\Sigma]]dW_t.$$

Finally, set $X_t = \exp\left(\widehat{x}_t\right)$ and note that

$$dX_t = \mathrm{diag}[X_t]\left(\mu^X(t, s_t^m, s_t^e)dt + \mathrm{diag}[\mathrm{dg}[\Sigma]]dW_t\right) \tag{5.23}$$

$$\mu^X(t, s_t^m, s_t^e) = K\left(\overline{\mu}^{\widetilde{X}} s_{t-}^m - \frac{1}{2}\mathrm{dg}\left[\Sigma\Sigma'\right] + \widetilde{A}(s_t^m)\frac{\mu^{p_w^e}(t, s_t^e)}{p_{wt}^e} 1_{\mathcal{E}_t}\right) + \frac{1}{2}\mathrm{dg}[\mathrm{dg}[\Sigma]\mathrm{dg}[\Sigma]']. \tag{5.24}$$

This establishes the one-to-one mapping between underlying and orthogonalized macro factors in (2.8), (2.9), (2.10). With $A(s_t^m) = [A^C(s_t^m), A^G(s_t^m), A^Y(s_t^m)]$, the relations are $A(s_t^m) = K\widetilde{A}(s_t^m)$, $\mu_o^X(s_t) = K\left(\mu^{\widetilde{X}} s_{t-} - \frac{1}{2}\mathrm{dg}\left[\Sigma\Sigma'\right]\right) + \frac{1}{2}\mathrm{dg}[\mathrm{dg}[\Sigma]\mathrm{dg}[\Sigma]']$ and $\Sigma_{ij}^X = 1_{\{i=j\}}\mathrm{dg}[\Sigma]_i$. The last relation shows $\sigma^C = \sigma^C$, $\sigma^G = \sigma^D\sqrt{1 - (\rho^{CD})^2}$ and $\sigma^Y = \sigma^E\sqrt{1 - (\rho^{CE})^2 - (\rho^{DE})^2}$.

## References


[1] Berrada, T., Detemple, J. and M. Rindisbacher (2018). Asset Pricing with Beliefs-Dependent Risk Aversion and Learning. *Journal of Financial Economics* 128(3), 504–534.

[2] Beeler, J. and J.Y. Campbell (2012). The Long-run Risks Model and Aggregate Asset Prices: an Empirical Assessment. *Critical Finance Review* 1(1), 141–182.

[3] Breeden, D.T. (1979). An Intertemporal Asset Pricing Model with Stochastic Consumption and Investment Opportunities *Journal of Financial Economics* 7(3), 265-296.

[4] Campbell, J.Y. and R.J. Shiller (1988). The Dividend-Price Ratio and Expectations of Future Dividends and Discount Factors. *Review of Financial Studies* 1(3), 195–228.

[5] Cheng. I.H. (2020). Volatility Markets Underreacted to the Early Stages of the COVID-19 Pandemic. *Review of Asset Pricing Studies* 10(4), 635–668.

[6] The COVID Tracking Project. https://covidtracking.com/data/national

[7] Cox, J.C., Ingersoll, J.E. and S.A. Ross (1985). A Theory of the Term Structure of Interest Rates, *Econometrica* 53(2), 385–407.

[8] Detemple, J. (2022). Asset Prices and Pandemics: The Effects of Lockdowns. *Quarterly Journal of Finance*. https://doi.org/10.1142/S201013922240002X

[9] Eichenbaum, M.S., Rebelo, S. and M. Trabandt (2021). The Macroeconomics of Epidemics. *Review of Financial Studies* 34(11), 5149–5188.

[10] Gormsen, N.J. and R.S.J. Koijen (2020). Coronavirus: Impact on Stock Prices and Growth Expectations, *Review of Asset Pricing Studies* 10(4), 574–597.

[11] Harvey, C.R. (1988). The Real Term Structure and Consumption Growth. *Journal of Financial Economics* 22(2), 305–333.

[12] Hong, H., Wang, N. and J. Yang (2021). Implications of Stochastic Transmission Rates for Managing Pandemic Risks. *Review of Financial Studies* 34(11): 5224–5265.

[13] Jones, C.J., Philippon, T. and V. Venkateswaran (2021). Optimal Mitigation Policies in a Pandemic: Social Distancing and Working from Home. *Review of Financial Studies* 34(11): 5188–5223.

[14] Merton, R.C. (1973), An Intertemporal Capital Asset Pricing Model. *Econometrica* 41(5), 867-887.

[15] Ogaki, M. (1993). Generalized Method of Moments: Econometric Applications. *Handbook of Statistics* 11, 455–488.

[16] Politis, D.N. and J.P. Romano (1994). Large Sample Confidence Regions Based on Subsamples under Minimal Assumptions. *Annals of Statistics* 22(4), 2031–2050 .